CO_2 MOBILITY CONTROL USING DIRECT THICKENERS AND FOAMING AGENTS

by

Dazun Xing

B.S in Chemical Engineering, Dalian University of Technology, 2007

Submitted to the Graduate Faculty of

Swanson School of Engineering in partial fulfillment

of the requirements for the degree of

Doctor of Philosophy

University of Pittsburgh

2012

UNIVERSITY OF PITTSBURGH

SWANSON SCHOOL OF ENGINEERING

This dissertation was presented

by

Dazun Xing

It was defended on

November 26th, 2012

and approved by

Karl Johnson, PhD, Professor, Department of Chemical and Petroleum Engineering

Sachin Velankar, PhD, Associate Professor, Department of Chemical and Petroleum Engineering

Yee Soong, PhD, Acting Division Director, National Energy Technology Laboratory

Dissertation Director: Robert Enick, PhD, Bayer Professor, Department of Chemical and Petroleum Engineering

CO_2 MOBILITY CONTROL USING DIRECT

THICKENERS AND FOAMING AGENTS

Dazun Xing, PhD

University of Pittsburgh, 2012

There are two strategies for using CO_2-soluble compounds to decrease the mobility of supercritical carbon dioxide. The first involves the "direct thickening" of CO_2, which is accomplished by dissolving an associative thickener in the $scCO_2$ that forms viscosity-enhancing macromolecules in solution. The second strategy is to inject a CO_2 surfactant solution into the porous media (which contains both brine and oil) that will generate a low mobility system of CO_2 droplets separated by surfactant-stabilized brine lamellae that bridge pore throats.

Direct thickening was accomplished with surfactants that formed cylindrical, rather than spherical, micelles in $scCO_2$. The surfactants employed divalent cations (Ni, Co) rather than a monovalent cation (Na). Therefore, each surfactant had two tails (rather than one). Further, each tail was a double-tail or triple-tail that was tailored to be CO_2-philic, consisting of either highly fluorinated alkanes or highly branched hydrocarbon groups. High pressure SANS was employed to establish whether the micelles were cylindrical or spherical. Further, the dimensions of the micelles were determined. Cloud point pressures of surfactant solutions (1-10wt% surfactant) were determined for the dry and wet (W=0–15, water/surfactant molar ratio) systems using a non-sampling technique, and viscosity was determined using a falling cylinder technique. The CO_2 viscosity was doubled using several weight percent of a fluorinated surfactant in the presence of water.

Several commercially available, nonionic surfactants were identified that are capable of dissolving in carbon dioxide (CO_2) in dilute concentration at typical minimum- miscibility-pressure (MMP) conditions and, upon mixing with brine in a high-pressure windowed cell, stabilizing CO_2-in-brine foams. These slightly CO_2- soluble, water-soluble surfactants include branched alkylphenol ethoxylates, branched alkyl ethoxylates, a fatty-acid-based surfactant, and a predominantly linear ethoxylated alcohol. Many of the surfactants were between 0.02 to 0.06 wt% soluble in CO_2 at 1,500psi and 25ºC, and most demonstrated some capacity to stabilize foam. The most- stable foams observed in a high-pressure windowed cell were attained with branched alkylphenol ethoxylates, several of which were studied in transient mobility tests using Berea sandstone cores, and high-pressure computed-tomography (CT)-imaging tests using polystyrene cores. The in-situ formation of weak foams was verified during transient mobility tests by measuring the pressure drop across a Berea sandstone core as a CO_2/surfactant solution was injected into a Berea sandstone core initially saturated with brine; the pressure-drop values when surfactant was dissolved in the CO_2 were at least twice those attained when pure CO_2 was injected into the same brine-saturated core. The greatest mobility reduction was achieved when surfactant was added both to the brine initially in the core and to the injected CO_2.

TABLE OF CONTENTS

PREFACE XIV

1.0 INTRODUCTION 1

1.1 ENHANCED OIL RECOVERY 1

1.2 SUPERCRITICAL CO_2 IN EHANCED OIL RECOVERY 2

1.3 PROBLEMS WITH CO_2 FLOODING 3

1.4 PREVIOUS WORK ON CO_2 DIRECT THICKENERS 5

1.5 CO_2 MOBILITY CONTROL BY FOAMING AGENTS 7

2.0 EXPERIMENTAL APPARATUS 14

2.1 PHASE BEHAVIOR APPARATUS 14

2.2 FALLING VISCOMETER APPARATUS 16

2.3 FOAM STABILITY APPARATUS 17

2.4 CO_2 MOBILITY TEST UNIT 19

3.0 RESULTS OF DIRECT THICKENERS 21

3.1 SELF-ASSEMBLY FLUORINATED DI-CHAIN SURFACTANTS 22

3.1.1 Phase behavior results of fluorinated Co, Ni, di-chain surfactants 24

3.1.2 Viscosity enhancement results of Self-assembly fluorinated di-chain surfactants 26

3.2 ALUMINUM DI-SOAPS 28

3.2.1 Synthesis of aluminum di-soaps 29

3.2.2 Solubility results of aluminum di-soaps in hexane 32

3.3 VISCOSITY RESULTS FOR 2-ETHYL-HEXANOIC ACID 34

4.0 RESULTS OF FOAMING AGENTS 35

4.1 BRANCHED ALKYLPHENOL ETHOXYLATES 38

4.1.1 Sigma-Aldrich Triton X-100, Huntsman Surfonic OP 100, and BASF OP 10 38

4.1.1.1 Solubility results of Triton X-100, Huntsman Surfonic OP 100, and BASF OP 10 39

4.1.1.2 Foam stability results of Triton X-100, Huntsman Surfonic OP 100 and BASF OP 10 40

4.1.2 DOW Tergitol NP series 41

4.1.2.1 Solubility results of DOW Tergitol NP series 41

4.1.2.2 Foam stability results of DOW Tergitol NP series 43

4.1.3 Huntsman's Surfonic N series 44

4.1.3.1 Solubility results of Huntsman's Surfonic N series 44

4.1.3.2 Foam stability results of Huntsman's Surfonic N series 46

4.1.4 Other branched alkylphenol ethoxylates 47

4.1.4.1 Structures of other branched alkylphenol ethoxylates 47

4.1.4.2 Solubility results of other branched alkylphenol ethoxylates 49

4.1.4.3 Foam stability results of other branched alkylphenol ethoxylates . 50

4.2 BRANCHED ALKYL ETHOXYLATES 52

4.2.1 Structures of branched alkyl ethoxylatyes 52

4.2.2 Solubility results of branched alkyl ethoxylatyes 54

4.2.3 Foam stability results of branched alkyl ethoxylatyes 57

4.3 FATTY ACID-BASED SUFACTANTS AND LINEAR ALYKYL ETHOXYLATES 59

4.3.1 Structures of fatty acid-based surfactants and linear alkyl ethoxylatyes.. 59

4.3.2 Solubility results of fatty acid-based surfactants and linear alkyl ethoxylatyes..... 60

4.3.3 Foam stability results of fatty acid-based surfactants and linear alkyl ethoxylatyes..... 62

4.4 EFFECT OF CO_2: BRINE VOLUMETRIC RATIO ON THE FOAM STABILITY 64

4.5 FOAM STABILITY RESULTS WITH SACROC BRINE 65

5.0 CO_2 MOBILITY CONTROL RESULTS OF CO_2-FLOODING THROUGH POROUS MEDIA EXPERIMENTS..... 69

6.0 CT IMAGING RESULTS OF CO_2 INVADING BRINE-SATURATED POLYSTYRENE CORE..... 74

7.0 SUMMARY AND CONCLUSION..... 77

8.0 FUTURE WORK 80

APPENDIX A..... 82

APPENDIX B 83

APPENDIX C 84

APPENDIX D 85

BIBLIOGRAPHY..... 86

LIST OF TABLES

Table 1. Solubility results of aluminum di-soaps in hexane 32

Table 2. Solubility results of aluminum di-soaps in CO_2 33

LIST OF FIGURES

Figure 1. a) Ideal flow of CO_2 from injection well (I) to Production well (P) for maximum oil recovery b) Viscous fingering of CO_2 leaving behind large volume of oil trapped 4

Figure 2. Early breakthrough of CO_2 resulting in low areal and vertical sweep efficiencies..... 4

Figure 3. Stucture of polyfluoroacrylate-styrene copolymer..... 6

Figure 4. Schematics of Robinson Cell..... 14

Figure 5. Quarts cylinder and floating piston 16

Figure 6. Illustration of falling cylinder viscometry..... 17

Figure 7. Illustration of foam forming and collapsing..... 18

Figure 8. CO_2 flooding through porous media apparatus 19

Figure 9. Structure of fluorinated monovalent surfactant, Na(di-HCF4) 23

Figure 10. Structure of fluorinated divalent surfactants,$Co(di\text{-}HCF4)_2$ and $Ni(di\text{-}HCF4)_2$ 23

Figure 11. Phase behavior result of fluorinated sodium surfactant, w=0, T=25°C 24

Figure 12. Phase behavior of fluorinated nickel surfactant, w=0, T=25°C 25

Figure 13. Phase diagram comparing effect of surfactant concentration and W on the stability of $Co(di\text{-}HCF4)_2$ surfactant in CO_2 at 25 °C. Point marked x represents a repeat conducted, with the same surfactant batch, but in a different cell and by a different operator..... 26

Figure 14. High-pressure viscosity measurements at 25°C, 350 bar and w = 10 showing the effect of surfactant counterion on relative viscosity η_{mic}/η_{CO2}, the ratio of microemulsion viscosity (η_{mic}) compared to that for neat CO_2 (η_{CO2}) 28

Figure 15. General structures of aluminum di-soaps..... 28

Figure 16. Structure of hydroxyaluminum di-2-ethyl-hexanoic tail soap..... 30

Figure 17. Structure of hydroxyaluminum di-3,5,5-trimethyl hexanoic tail soap 30

Figure 18. Structure of hydroxyaluminum di-pivilic tail soap 30

Figure 19. Structure of hydroxyaluminum di-terbutyl acetic tail soap..... 30

Figure 20. General synthesis procedures of aluminum di-soaps 31

Figure 21. Structure of hydroxyaluminum di-isostearate-N soap..... 33

Figure 22. Structure of hydroxyaluminium di-(4-methylvalerate) soap..... 33

Figure 23. High-pressure viscosity measurements for 2-ethyl-hexanoic acid at 25°C, 5000psi .. 34

Figure 24. Structure of Sigma-Aldrich Triton X-100, Huntsman Surfonic OP 100, and BASF OP 10, n=9~10 38

Figure 25. Solubility of Triton X-100, Huntsman OP 100 and BASF OP 10 in CO_2 at 25ºC..... 39

Figure 26. 0.04wt% Triton X-100, Huntsman OP 100, and BASF OP 10 in CO_2 at 1300psi and 25 ºC, with a brine (5wt%NaCI)/CO_2 volume ratio 1:1 40

Figure 27. Structure of DOW NP Series, x = 4,6,9,12,15 (alkyl chain structure is proprietary; this is a qualitative representation) 41

Figure 28. The solubility of NP series in CO_2 at 25ºC, also NP 9 and NP 15 at 58ºC 41

Figure 29. 0.04wt% NP9, 0.03wt% NP12 and NP15 surfactants in CO_2 at 1300psi and 25ºC, with a brine(5wt%NaCI)/CO_2 volume ratio 1:1 43

Figure 30. Structure of Huntsman Surfonic N series, x = 8.5, 9.5, 10, 12, 15, 20, 30, 40..... 44

Figure 31. The solubility of Huntsman N series surfactants in CO_2 at 25 ºC..... 44

Figure 32. The solubility of Huntsman N series surfactants in CO_2 at 58 ºC..... 45

Figure 33. The foam stability associated with the Huntsman Surfonic N series foams at 1300psi and 25 ºC, with a brine(5wt%NaCI)/CO_2 volume ratio 1:1; 0.04wt% N85, 0.03% N120 and N150, N200. Control results for water soluble Chaser CD 1045 at a concentration of 0.04wt% are also shown..... 46

Figure 34. Structures of huntsman Surfonic DDP 100 (x = 10) and 120 (x = 12)..... 47

Figure 35. Structures of huntsman Surfonic dinonylphenol DNP 150 (x = 15) and 180 (x = 18) 47

Figure 36. Structure of huntsman Surfonic N (PO1) 100 (n=10) 48

Figure 37. Structure of huntsman TSP 15, tristyrylphenol ethoxylates (n=15) 48

Figure 38. The solubility of Huntsman DNP150, 180, DDP 100, 120, TSP, Surfonic N(PO1) 100, Stepan Cedepal CO 630 and CO 710 in CO_2 at 25ºC 49

Figure 39. 0.03wt% Stepan CO 710 and CO 630 in CO_2 at 1300psi and 25ºC, with a brine (5wt%NaCl)/CO_2 volume ratio 1:1 50

Figure 40. 0.03wt% Huntsman DDP 120 and DNP 150 in CO_2 at 1300psi and 25ºC, with brine (5wt%NaCl)/CO_2 volume ratio 1:1 50

Figure 41. The foam stability of 0.03wt%, 0.04wt% Huntsman Surfonic N(PO1) 100 in CO_2 at 1300psi and 25°C, with a brine (5wt%NaCI)/CO_2 volume ratio 1:1 51

Figure 42. The foam stability of 0.03wt%, 0.04wt% and 0.05wt% Huntsman TSP 15, tristyrylphenol ethoxylates in CO_2 at 1300psi and 25°C, with a brine (5wt%NaCI)/CO_2 volume ratio 1:1 51

Figure 43. Structure of Dow trimethylnonyl Tergitol TMN 6 (x = ~8) 52

Figure 44. Structures of BASF Lutensol XP 70 (x = 7) and 80 (x = 8) (Guerbet alcohol-based C10 alkyl chain structure is proprietary, the structure above is our qualitative representation) .. 53

Figure 45. Structures of BASF Lutensol TO 8 and 10 iso C13 oxoalcohol ethoxylates and 8 or 10 EO groups (the structure above is our qualitative representation) 53

Figure 46. Structures of Huntsman isotridecyl ethoxylate TDA 8, TDA 9, TDA 11, x=8, 9 ,11 respectively, branched tridecyl alcohol ethoxylates with multiple methyl and/or ethyl branches on alcohol alkyl groups 53

Figure 47. The solubility of TMN 6 and BASF XP 70 in CO_2 at 25ºC and 58ºC, XP 80 in CO_2 at 25ºC 54

Figure 48. The solubility of BASF Lutensol TO 8, 10 and Huntsman TDA 8, 9 and 11 in CO_2 at 25 ºC 54

Figure 49. The solubility of BASF Lutensol TO 8, 10 and Huntsman TDA 8, 9 and 11 in CO_2 at 58ºC 55

Figure 50. The foam stability of 0.04wt% BASF Lutensol XP 70 and BASF Lutensol XP 80 in CO_2 at 1300psi and 25 ºC, with a brine (5wt%NaCI)/CO_2 volume ratio 1:1 57

Figure 51. The foam stability of 0.03wt% BASF TO 8, 10, 0.03wt% and 0.04wt% Huntsman TDA 8, 0.03wt% Huntsman TDA 9, and 0.1wt% Huntsman TDA 11 in CO_2 at 1300psi and 25ºC, with a brine(5wt%NaCI)/CO_2 volume ratio 1:1 58

Figure 52. Structure of Monolaurate polyethyleneglycol, Sigma Aldrich PEG monolaurate 600 (x = 9) 59

Figure 53. Structure of Sigma Aldrich Polyoxyethylene (20) sorbitan monooleate, Tween 80... 59

Figure 54. Structures of Huntsman L 12-8, the eight-mole ethoxylates of linear, primary C10-12 alcohol, (x ~ 12, y = 8), BASF Lutensol AO 8, AO 11, (x ~ 13.7, y = 8, 11), saturated, predominantly unbranched C_{13-15} oxo alcohol that consists of 67% C_{13} and 33% C_{15}..... 60

Figure 55. The solubility of Huntsman L 12-8, BASF AO 8, 11, Sigma Tween 80 and PEG monolaureate in CO_2 at 25 ºC 60

Figure 56. The foam stability of Sigma Tween 80 in CO_2 at 1300psi and 25ºC, with a brine (5wt%NaCI)/CO_2 volume ratio 1:1 62

Figure 57. The foam stability of 0.03wt% BASF AO 8 and AO 11 in CO_2 at 1300psi and 25 ºC, with a brine (5wt%NaCI)/CO_2 volume ratio 1:1 63

Figure 58. Effect of CO_2: brine volumetric ratio on the foam stability test, the volumetric ratio is provided in the parentheses of the legend. The solid lines represent the top of the emulsion phase, while the dashed curves represent the bottom of the emulsion phase. 64

Figure 59. The foam stability of 0.05% and 0.2wt% Huntsman N 150 in CO_2 at 3200psi and 58°C, with SACROC/CO_2 brine volume ratio 1:1 66

Figure 60. The foam stability of 0.05% and 0.1wt% Huntsman TDA 11 in CO_2 at 3200psi and 58°C, with SACROC brine/CO_2 volume ratio 1:1 67

Figure 61. The foam stability of 0.03wt% Huntsman N 200, Huntsman N 300, Huntsman N 400, and BASF TO 10 in CO_2 at 3200psi and 58ºC, with SACROC brine/CO_2 volume ratio 1:1 68

Figure 62. Photograph of the NETL mobility apparatus 71

Figure 63. Pressure drop across a 6" long, 1"diameter, 104 md Berea sandstone core, 25ºC, ~2700 psi, 1 cm^3/min volumetric flow rate (superficial velocity of 10ft/day) 72

Figure 64. Medical CT scanner at NETL with core holder and flow pumps..... 74

PREFACE

I would like to express my deepest gratitude to my advisor, Dr. Robert Enick for his encouragement, guidance and assistance throughout this research. I have learned considerable amount of research knowledge and techniques, also spiritually, he always offers his unconditional support to my work. I would like to extend my gratitude to committee members, Dr. Karl Johnson, Dr. Sachin Velankar, and Dr. Yee Soong, for their time on my proposal and PhD defense.

I would like to thank Dr. Julian Eastoe and his research group from University of Bristol, UK, for our pleasurable collaboration on CO_2 direct thickener project.

I would like to express my special thanks to Yee Soong and his colleagues in National Energy Technology Laboratory, for his help on setting up the whole CO_2-flow-through porous media apparatus for my experiments.

I would show great appreciation to my lab mates, Matt Miller, Bing Wei, Xin Fan, Katherine Barillas, James Mclendon, Lei Hong, Sam McNulty and Peter Koronaios, for their helpful discussions and exchange of ideas, as well as for the good time they brought to my work at University of Pittsburgh.

Last but not the least; I would like to acknowledge National Energy Technology Laboratory for the financial support throughout my PhD.

1.0 INTRODUCTION

Two important processes [1] in the oil and gas industry that use dense carbon dioxide are fracture stimulation and enhanced oil recovery. For enhanced oil recovery, the problems with using carbon dioxide have been well studied and documented in laboratory and field studies. The low viscosity of carbon dioxide causes it to 'finger' towards the production wells and bypass large amounts of oil. Significant research has been conducted over the past 30 years searching for ways to increase the viscosity of (thicken) carbon dioxide.

1.1 ENHANCED OIL RECOVERY

Recent reports [2] from the US DOE suggest that in total there is 1,332 billion barrels of domestic oil resources which include original, developed and undeveloped fields. Out of this only 208 billion barrels is recovered by primary and secondary recovery. An additional 400 billion barrels can be technically recovered by using present enhanced oil recovery techniques. There are 724 billion barrels of unrecoverable oil in place; new technologies must be developed for the recovery of this portion.

Oil recovery techniques have been grouped into three basic categories: primary, secondary and tertiary oil recovery. Primary recovery techniques exploit the pressure within the reservoir to drive oil from the porous medium to surface from production wells with the

assistance of production pumps (if necessary). When the reservoir natural pressure becomes too low to maintain economical production rate, then secondary recovery methods are applied. In secondary recovery, an external force is applied to drive the oil to production well. This is typically done by injecting high pressure water or nitrogen into the reservoir. On average, the recovery of original oil after primary and secondary recovery operations is between 30 to 40%, depending upon reservoir characteristics. Tertiary or enhanced oil recovery (EOR) is usually initiated near the end of economical secondary recovery to maintain oil production rates and thereby increase the amount of oil ultimately recovered from the reservoir. It typically involves injecting of supercritical CO_2 ($scCO_2$), steam, polymer solutions, sodium hydroxide solutions or surfactant solutions to improve oil flow from the reservoir.

1.2 SUPERCRITICAL CO_2 IN EHANCED OIL RECOVERY

High pressure liquid CO_2 in EOR has been used by oil industry well over 50 years. CO_2 flooding has gained attention as one of the most technologically viable means of recovering undeveloped oil in place. CO_2 flooding efficiency strongly depends on reservoir temperature, pressure and crude oil composition.

For practical proposes CO_2-EOR is divided into two processes: miscible displacement and immiscible displacement. Miscible CO_2 displacement takes place under favorable temperature, pressure and crude oil composition, at which CO_2 become miscible with crude oil after the extraction of the lighter ends of crude oil near the injection well. Naturally, CO_2 is not miscible with oil on first contact. However, displacement tests in long cores and sand packed slim tubes indicate that dynamic displacement is possible above minimum miscibility pressure

(MMP) [3] (the pressure at which oil recovery is essentially complete i.e. compressing CO_2 above MMP does not result in increase in additional oil recovery). When CO_2 is injected and is brought in contact with crude oil, initially its composition is enriched with vaporized intermediate components of the oil. This local change in the composition near the injection well results in the development of a miscible zone between oil and CO_2, within a relatively short distance from the injection well. For the effective mixing of oil and CO_2, this process should take place above MMP. The value for MMP depends on reservoir temperature, pressure and crude properties. This CO_2-oil interaction makes oil swell and reduces its viscosity. As a result it improves the oil recovery rate and ultimate amount of oil recovery (relative to continued water flooding).

Immiscible CO_2 displacement takes place when the reservoir pressure is below the MMP or the crude oil is not miscible with CO_2, typically because the reservoir is so shallow that it cannot withstand the MMP requirement. Even when crude oil is not miscible with CO_2, increased oil recovery occur due to oil viscosity reduction, oil swelling and reduction in surface tension [4].

1.3 PROBLEMS WITH CO_2 FLOODING

Theoretically, nearly all the oil remaining in the reservoir after a CO_2 flood could possibly be recovered if it is swept by the CO_2 at the MMP, but in the field recovery is limited to about 20% of the original oil in place (OOIP). Reasons for this low recovery are:

1. Unstable flow (fingering, shown in Figure 1) of CO_2: i.e. CO_2 is more mobile than oil or water being displaced. (Mobility is permeability/viscosity.) Early breakthrough of CO_2 results

in CO_2 coming out of production well long before all the oil is removed due to high CO_2 mobility. (shown in Figure 2)

2. Low density of CO_2 (at MMP) relative to oil causes gravity override, which inhibits the contact of CO_2 with oil in the lower portion of reservoirs.

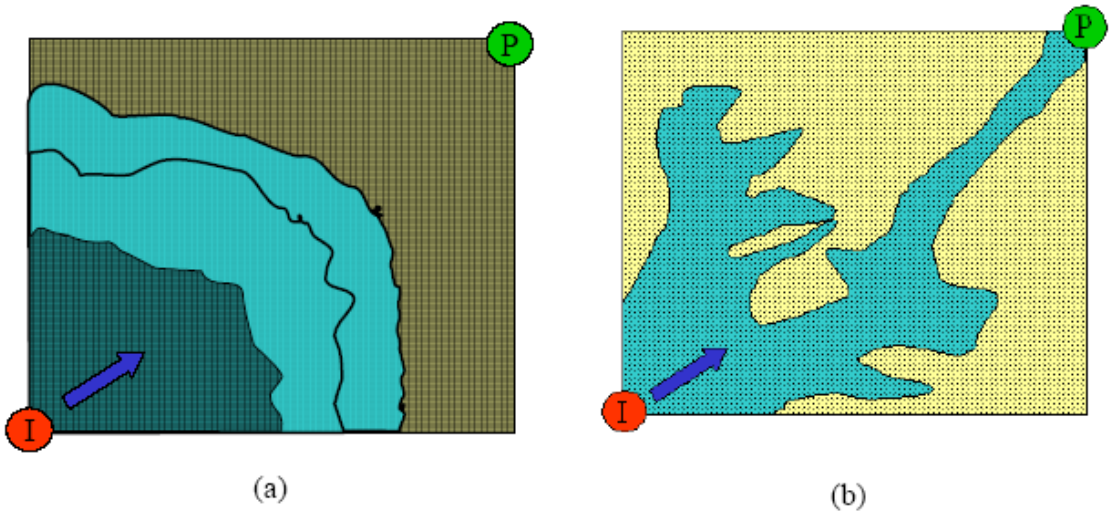

Figure 1. a) Ideal flow of CO_2 from injection well (I) to Production well (P) for maximum oil recovery b) Viscous fingering of CO_2 leaving behind large volume of oil trapped

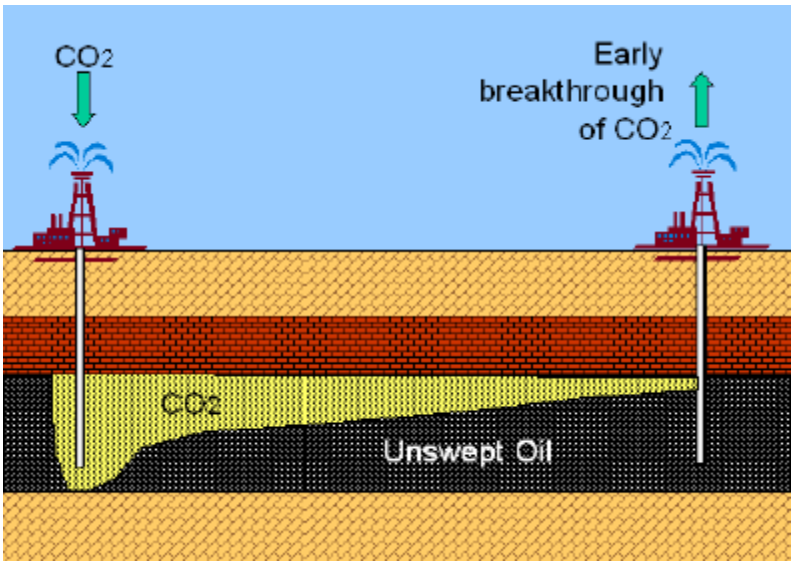

Figure 2. Early breakthrough of CO_2 resulting in low areal and vertical sweep efficiencies

It is not practical to increase the density of CO_2 by several tenths of a g/cc at a specified temperature and pressure via use of dilute concentration of additives, nor is it feasible to significantly decrease the permeability of CO_2 in the formation without introducing large volumes of brine (WAG) [1]. It is conceivable, however, to make significant increase in viscosity via the introduction of dilute amounts of a thickener (oil and water thickeners that are effective at concentrations of 0.1-1wt% are commonplace).

1.4 PREVIOUS WORK ON CO_2 DIRECT THICKENERS

Based on the results of Jianhang Xu, form Dr. Robert Enick's research group [5], among all the possible thickeners, fluoroacrylate-styrene copolymer (29% styrene and 71%fluoroacrylate monomer) gave the most significant viscosity enhancement. Most of their work was done under typical reservoir condition. (20Mpa, 20~100°C, 1ft/day or 10ft/day for superficial velocity) 5wt% of the copolymer enhances CO_2 viscosity by a factor of 200, even in 1.5wt% copolymer and CO_2 solution, relative viscosity is increased several times. The minimum concentration to give appreciable viscosity enhancement is about 0.2wt%. The fluoroacrylate functionality is highly CO_2-philic, so that the copolymer does not need a co-solvent for dissolution in CO_2. The styrene provides the intermolecular "π-π" stacking of benzene rings, which induce the CO_2-thickening process, meanwhile, the increase of the styrene group led to the decrease of the solubility in CO_2. The composition balance between fluoroacrylate and styrene is required, which was finally determined to be 71wt% of the fluoroacrylate and 29wt% of the styrene. They also mentioned that temperature effect almost did not affect the viscosity enhancement, while the

increase of shear rate lowered the relative viscosity, because of the copolymer's shear-thinning nature.

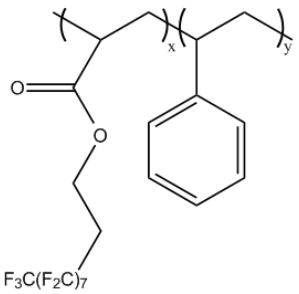

Figure 3. Stucture of polyfluoroacrylate-styrene copolymer

The PolyFAST copolymer is the first success "direct thickener", since no other co-solvent is required. Unfortunately, such copolymers are expensive, unavailable in large scale, and environmentally persistent, in terms of their highly fluorinated nature. New development and design of "direct thickener" is one of our research priorities. We are still trying to discover or design inexpensive and biodegradable direct thickeners available in large quantities either by synthesis or through commercial purchase. The new generation of direct thickeners should primarily consist of carbon, hydrogen, oxygen and nitrogen. Meanwhile, the CO_2-philic group and the viscosity- enhancing group should be also proportionally integrated in the same direct thickener. Most of the time, it is almost impossible that a non-fluorinated direct thickener can be designed because the most CO_2-philic, high molecular weight, non-fluorinated polymers (e.g. polyvinyl acetate) or functional groups require the pressures that are many thousands of psi above the MMP to dissolve, while they also will become much less CO_2-philic upon the inclusion of CO_2-phobic associating groups required for viscosity-enhancing intermolecular associations to occur. In a word, it is extremely hard to find a balance between high solubility and strong ability to promote the CO_2 viscosity.

1.5 CO_2 MOBILITY CONTROL BY FOAMING AGENTS

The notion of dissolving a surfactant into liquid CO_2 during an enhanced oil recovery process for the purpose of generating CO_2-in-brine mobility-control foams was suggested by Bernard and Holm in their 1967 patent [6]. In particular, they suggested the use of a branched octylphenol ethoxylate, Triton X-100, at a concentration of 1wt% in CO_2 at 80^{o}F (26.7^{o}C) and 1000psi (~6.9MPa). However, dense CO_2 is a feeble solvent for polar compounds and Triton X-100 is not nearly soluble in CO_2 at such concentration. The difficulty in dissolving surfactants in CO_2 did not escape the attention of Irani [7], who in 1989 suggested that a co-solvent could be added to the CO_2 in an attempt to dissolve siloxane-based surfactants, which have very low solubility parameters. In 1991, Schievelbein [8] suggested the use of hydrocarbon-based surfactants without the use of a co-solvent. In his summary, Schievelbein recommended using at least 0.2wt% (2000 ppm) of an ethoxylated alkyl or ethoxylated alkyl-aryl (i.e. alkylphenol) hydrocarbons that contain an alkyl chain with an average of 7 to 15 carbons and an average of between 1 to 7 ethoxide (i.e. ethylene oxide or EO) units. Typically, surfactants with such short EO tails are likely to be water-insoluble or water-dispersible, making them unlikely to stabilize CO_2-in-water or CO_2-in-brine emulsions. Bancroft's rule states [9] that the surfactant should be more soluble in the continuous phase (aqueous films) than the high-volume discontinuous phase (dense CO_2) for an emulsion or foam to be stabilized. Further, it may be difficult for these surfactants with very short EO segments to attain CO_2 solubility values of 2000 ppm or more at typical reservoir MMP conditions.

There was a great deal of interest in the identification and design of CO_2-soluble surfactants for chemical engineering applications during the last three decades. Although most of this work was directed at the identification of CO_2-soluble surfactants that could stabilize water-

in-CO_2 microemulsions for chemical engineering applications, a portion of the research was aimed at the stabilization of CO_2-in-water/brine foams at supercritical CO_2 conditions and emulsions at liquid CO_2 conditions. For example, Johnston and coworker (Dhanuka 2006) [10] noted that DOW Tergitol TMN 6 (Mw = 552) poly(ethylene glycol)$_{8.33}$, 2,6,8-trimethyl-4-nonyl ether (90% active, 10%water) was an effective foaming agent. Tergitol TMN 6 was added at a concentration of 5wt% of the water mass to a mixture of 90vol%CO_2 and 10vol% water (roughly 0.5wt% Tergitol TMN-6 based on the CO_2 mass). After being agitated by a stirrer and a recirculation pump, very stable (more than 2 days) white, opaque foams formed at 25^{o}C and pressures of 207 bar and 345 bar. The bubbles were roughly 10 microns in size. An excess water phase slowly formed at the bottom of the cell as the water of the lamellae slowly drained by gravity. No excess CO_2 appeared above the foam at top of the windowed cell (which would have been formed by bubble coalescence) was observed. In an earlier paper (Ryoo 2003) [11], Johnston and coworkers determined the solubility of several TMN surfactants of varying ethoxylate chain length, TMN 3, 6, 10 (3, 8.33, 12 EO groups respectively); they were all soluble at 1wt% at temperatures between 25-75^{o}C at pressures of ~80-300 bar, with increasing pressure required for increasing EO length and increasing temperature. Haruki and co-workers (2007) [12] studied the phase behavior of TMN 3 (with 5 EO groups) at temperatures between 308-343K and concentrations between ~0.5-3.0wt%. These results indicated that Johnston's experiments were conducted at conditions where the surfactant could have been completely dissolved in the CO_2 phase, therefore Tergitol TMN 6 is a viable candidate for dissolution into the CO_2 being used for miscible flooding. Johnston and co-workers [11] also established that at 40^{o}C the linear alkyl ethoxylates with the same number of carbon atoms (i.e. the Nikko linear alkyl isomers of the DOW branched TMN surfactants) were less CO_2 soluble than branched analogs; although this

difference was significant for concentrations between 5-45wt% surfactant, the difference became very small at concentrations less than 5wt%. This finding is in agreement with the well documented conclusions of Eastoe and coworkers that branching of an alkyl tail (e.g. incorporation of multiple methyl groups along the alkyl chain, incorporation of t-butyl tips) can significantly enhance the CO_2 solubility of hydrocarbon-based surfactants [13-17]. Johnston and co-workers (daRocha 2001) [18] investigated the ability of di-block and tri-block surfactants with siloxane-based, fluorocarbon-based and polyalkyloxide-based CO_2-philic segments to stabilize CO_2-in-water emulsions. A $(\text{butylene oxide})_{12}$-b-$(\text{ethylene oxide})_{15}$ diblock surfactant was particularly effective at forming emulsions that were stable for over 48 hours at temperatures between 25-65^{o}C, at very high pressures (e.g. 345 bar), and a concentration of 1wt% relative to equal masses of CO_2 and water (2wt% based on CO_2 alone). When water was used as the aqueous phase, the observed curvature (CO_2-in-water emulsion) was in accordance with that expected from Bancroft's rule because the surfactant is more soluble in water (1.2wt%) than CO_2(~0.1wt%) at these conditions. However, upon the addition of salt to the aqueous phase, CO_2-in-water emulsions continued to form even though the solubility of the surfactant in water became less than that in CO_2. Although this is not in accordance with Bancroft's generalized rule, it is a desirable attribute for the proposed EOR application. Both connate and injected aqueous phases are brine, and the ability of a surfactant to stabilize CO_2-in-water foams in the presence of substantial amounts of dissolved solids in the brine is critical to the success of the proposed technology. Therefore, $(\text{butylene oxide})_x$-b-$(\text{ethylene oxide})_y$ di-block surfactants may be viable candidates for stabilizing CO_2-in-brine foams or emulsions if it can be demonstrated that they are sufficiently soluble in CO_2 at injection and reservoir conditions and if they can

stabilize the foams at reservoir conditions. There are no current suppliers of these surfactants for large-scale oilfield applications, however.

Our research group established that oligo(vinyl acetate), oligo VAc, is extremely CO_2-philic, and suitable for incorporation into CO_2 soluble ionic surfactants [12]. Tan and Cooper [13] designed triblock VAc-b-EO-b-VAc surfactants capable of stabilizing CO_2 foams. In particular, a VAc30-EO60-VAc30 surfactant at a concentration of 1.6wt% based on the total mass of the system was able to form a stable emulsion (at least 48 hours) of CO_2-in-water at 20^oC and 200 bar. These emulsions contained as much as 97vol%CO_2; therefore the concentration of the surfactant on a CO_2 basis was ~1.5wt%. Due to the difficulty and expense associated with the synthesis of oligoVAc-based surfactants, however, it is very unlikely that these research surfactants will become commercially available in the immediate future.

In 2008, researchers from the University of Texas at Austin and Dow Oil & Gas used a proprietary surfactant dissolved at a concentration of 0.1wt% in CO_2 at ambient temperature in a mixing vessel at 1800 psi (~12.4MPa) to recover oil from a core with an effluent back pressure regulator of the core effluent set at 1500 psi (~10MPa) [19]. The investigators assessed various modes of surfactant injection including WAGS (water-alternating-gas with surfactant dissolved in the CO_2), SAG (surfactant-alternated-CO_2 with surfactant dissolved in the water) and continuous CO_2-dissolved-surfactant injection (no alternate injection of water used), and found that the injection of the CO_2-surfactant solution into the waterflooded core without the use of alternating water slugs yielded higher oil recovery that the other injection modes. Recently, the same type of surfactant was tested by Dow Oil & Gas in a SACROC pilot flood operated by Kinder Morgan [20]. The results indicated that a reduction in CO_2 injection at a constant pressure

occurred while 30% of the CO_2 was diverted into zones that had previously not seen CO_2. Both of these trends indicated that reduced-mobility CO_2-in-brine foams had formed in-situ.

Recently, the University of Texas at Austin and Dow Oil & Gas presented a study of the morphologies, stabilities, and viscosities of high-pressure carbon dioxide-in-water foams formed with water-soluble, branched, nonionic hydrocarbon surfactants that did not contain an aromatic or cyclic functionality [21]. In each case, the hydrophile was an ethoxylate group, designated as EO_n or EO_m,where n or m represented the number of repeat units in the PEG chain. Some surfactants contained a polypropylene oxide segment, designated as PO_n, between the hydrocarbon-based tail and the hydrophilic EO_n head group. PO_n is more CO_2-philic and less hydrophilic than the EO_n hydrophile. Surfactants that were examined include EO_n-PO_n-EO_n triblock copolymer, lauric acid-EO_{12}, 1-hexanol-PO_n-EO_m, 1-octanol-PO_n-EO_m, 2-octanol-PO_n-EO_m, 2-ethylhexanol-PO_n-EO_m, 2-ethylhexanol-$(EO_7PO_{5.5})_{random}$-EO, dodecyl/tetradecyl secondary-EO_n, TMN6 trimethylnonanol-EO_8, 1-nonanol-$PO_{3.5}$-EO_8, $C_{12-14}EO_7$ Brij surfactants, $H_3C(CH_2)_{x-1}$ PO_nEO_m, and dioctylglycerine-EO_n. The pressure was maintained at 13.8MPa (2000psi) and temperatures of 24, 40, 60 and 70^oC were considered. The synthetic brine was composed of 2%NaCl, 1%$CaCl_2$, and 0.5% $MgCl_2$ by weight. The volumetric ratio of the injected phases was 90% CO_2:10% surfactant solution. Because the concentration of the surfactant was 1wt% of the aqueous phase, the concentration of the surfactant relative to the CO_2 was about 0.13-0.25wt% over the 24-70^oC temperature range. The surfactant solubility in dense CO_2 was not presented, however. Foams were formed by dissolving the surfactant in the brine and then co-injecting this aqueous surfactant solution along with high pressure CO_2 into a sand pack with hydrophilic pores. Most of the surfactants did form foams at 24^oC, and the surfactants with the highest cloud point temperatures (the highest temperature at which a mixture of 1wt%

surfactant in the aqueous phase remains a single phase) yielded foams at the highest temperatures. For example the dodecyl/tetradecyl secondary-$EO_{20,}$ 1-hexanol-PO_5-EO_{15}, 2-ethylhexanol-PO_5-$EO_{15,}$ and 2-ethylhexanol- $EO_{11.5}$ surfactants all had cloud point values greater than 80^{o}C. These researchers presented another study [22] of the effect of surfactant branching on the interfacial properties at the CO_2-water interface (and air-water interface) using many of the same surfactants in their prior study [21].

Later on, the team of Dow Oil & Gas and Univ of Texas at Austin described a new, non-ionic, glycerin-based, twin-tailed, water-soluble, ethoxylated surfactant for stabilizing CO_2-in-water emulsions used for CO_2 flooding sweep improvement [23]. These surfactants, such as the dioctylglycerine-based surfactants with 9 or 12 EO units, DOG 9 and DOG 12, were more effective at reducing the CO_2-water interfacial tension to ~27mN/m, a value lower than other water-soluble surfactants such as the secondary alcohol based surfactants 15-S-7 and 15-S-12. DOG 9 and DOG 12 were also more effective at reducing the IFT than similar glycerine-based surfactants with shorter alkyl chains (such as the dibutylglycerine-based ethoxylates DBG 6 and DBG 10) and Brij surfactants $C_{12}E_7$ and $C_{12}E_{12}$. Although the solubility of these surfactants in CO_2 was not determined, these surfactants were subsequently dissolved in water and co-injected with pure CO_2 into cores. The general features of these novel surfactants make them likely candidates for dissolution in CO_2 or brine. Coreflooding tests were reported for a 2" diameter, 1' long carbonate core of ~ 80mD permeability at 45^{o}C initially saturated with 1% NaCl brine. Pure CO_2 was co-injected with a 0.2wt% brine solution at a 90:10 ratio and a superficial velocity of 1ft/day with the core effluent pressure maintained at 1500psi. Pressure drops realized during the experiments with DOG 9 were several times greater than those detected with aqueous solution of

15-S-7. This was indicative of lower mobility foams being generated with the novel dioctylglycerine ethoxylate than the secondary ethoxylated alcohol.

Johnston and co-workers also studied the use of a biocompatible, water-soluble, nonionic, ethoxylated surfactant, polyoxyethylene (20) sorbitan monooleate (polysorbate 80, Tween 80) for stabilizing CO_2-in-water and water-in-CO_2 emulsions and double-emulsions [24]. Tween 80 was reported to be CO_2 soluble to ~0.5–1.0wt% at pressures that are commensurate with MMP values. The Tween 80 surfactant was also capable of stabilizing emulsions containing micron-scale CO_2 bubbles generated by co-injecting aqueous surfactant solutions and CO_2 into sand packs.

All of these prior attempts to identify CO_2-soluble surfactants focused on non-ionic surfactants. Although ionic surfactants have been previously designed for solubility in CO_2, they typically require pressures far beyond the MMP. In an attempt to design CO_2-soluble, hydrocarbon-based, ionic surfactants that were extremely soluble in CO_2, Eastoe and co-workers developed a tri-chain, branched alkyl chain surfactant, sodium 1,4-bis(neopentyloxy)-3-(neopentyloxycarbonyl)-1,4-dioxobutane-2-sulfonate [25-26]. This surfactant, which is referred to Na TC14, is about 2wt% soluble in CO_2 at 25^{o}C and 2320psi [26]. These surfactants have yet to be assessed as foam-formers, however, and are expected to cost roughly 10 times as much as the commercially available surfactant AOT [25].

2.0 EXPERIMENTAL APPARATUS

In this part of the dissertation, the experimental apparatus used for phase behavior observation, viscosity enhancement of liquid CO_2 observation, foam stability observation, and core flooding observation are introduced, they are shown below, respectively.

2.1 PHASE BEHAVIOR APPARATUS

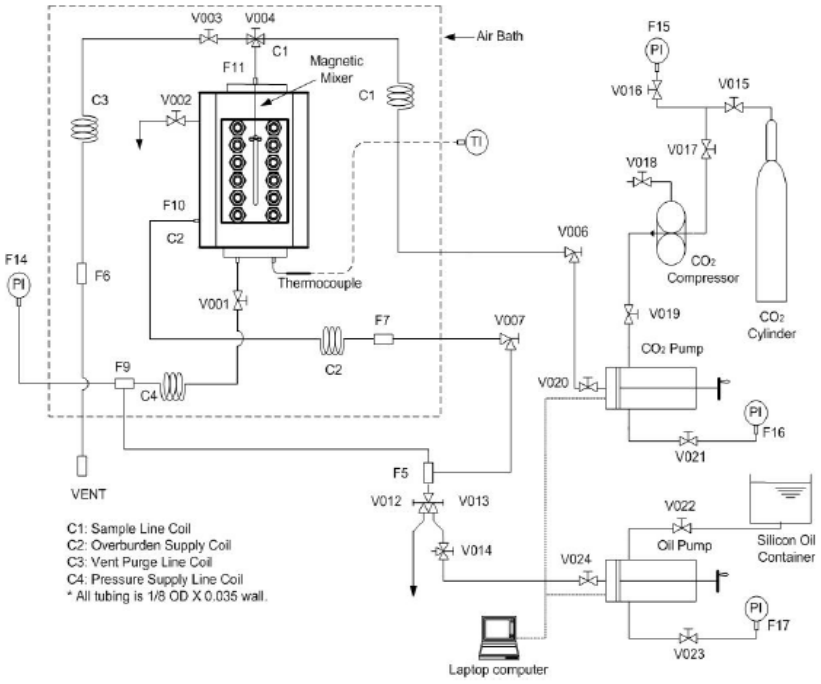

Figure 4. Schematics of Robinson Cell

Phase behavior studies were performed using high pressure, variable-volume, windowed cell. (D.B Robinson Cell, formerly DB Robinson and Associates, now Schlumberger) The system is retained in a constant temperature air bath, by which the temperature inside the Robinson Cell is controlled. The Cell temperature ranged from -10°C to 180°C and maximum pressure is 10000psi. The total volume of the cell is approximately 110 cc. For the phase behavior investigation, isothermal compression and expansion of CO_2 solution containing a certain sample of specified weight composition are used to determine solubility via cloud point determination. A calculated amount of sample is placed on top of the piston inside the glass cylinder. By compressing or expanding the overburden fluid (silicon oil), the piston correspondingly moves up or down, then changes the volume of the top chamber separated by the piston from the overburden fluid. The CO_2 liquid is then injected into the top chamber by a positive displacement pump while the top chamber volume is being expanded at the same volumetric rate as that of the withdrawal of the overburden oil. A desired amount of liquid CO_2 can be introduced into the top chamber in a smooth, isothermal, isobaric manner. The CO_2 solution is pressurized and mixed using magnetic stir until a clear single phase is observed at a certain pressure, meaning that the sample is dissolved in CO_2 solution.

The cell is slowly depressurized by expanding overburden fluid until the cloud point pressure is found. In CO_2 solution, when a certain sample starts separate from the CO_2 solution and a second phase may be observed as droplets of liquid or fine particles, which accumulate on the top of the piston, this pressure is considered to be the cloud point pressure. The same routine is repeated 3-4 times for each data collection. Bubble point pressure instantly observed when the first bubble of a CO_2-rich vapor appears.

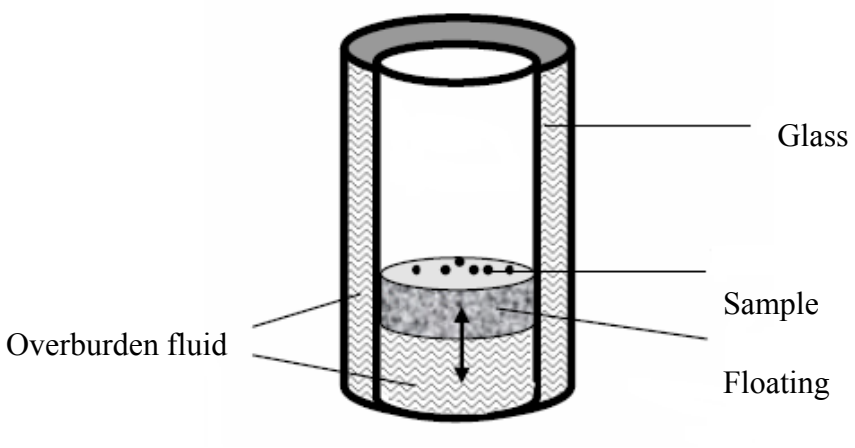

Figure 5. Quarts cylinder and floating piston

2.2 FALLING VISCOMETER APPARATUS

Falling cylinder viscometry is applied to measure the relative viscosity between the CO_2 solution with direct thickener and pure CO_2. Aluminum cylinders with 1-inch height and different diameters are used. The selected aluminum cylinder along with the thickening candidate is put on top of the moving piston, inside the glass cylinder, pressurized and stirred, until one single phase is reached. Once the single phase is steady and clear, the cell is inverted and the aluminum cylinder would fall in an almost constant velocity. The time for the cylinder falling is recorded, in order to calculate the terminal velocity, and then compare with that in pure CO_2 to evaluate the surfactants' thickening ability. Within the whole length of the glass cylinder, only several centimeters are timed during the whole process, since a steady movement and a constant velocity of the aluminum cylinder need to be guaranteed. This procedure is repeated approximately 10 times to acquire consistent and valid data. Before a certain candidate is tested for thickening

ability, the aluminum cylinder falling velocity in pure CO_2 under same condition (pressure, temperature) needs to be determined.

The relation between the velocity of falling cylinder and viscosity of CO_2 is derived from Navier-Stokes equation with following assumptions:

- The cylinder and glass tube are coaxial and concentric.
- The compressibility of fluid is low during the experiment.
- Density difference of the fluid above and below the piston is negligible
- Temperature and pressure are maintained constant during the experiment

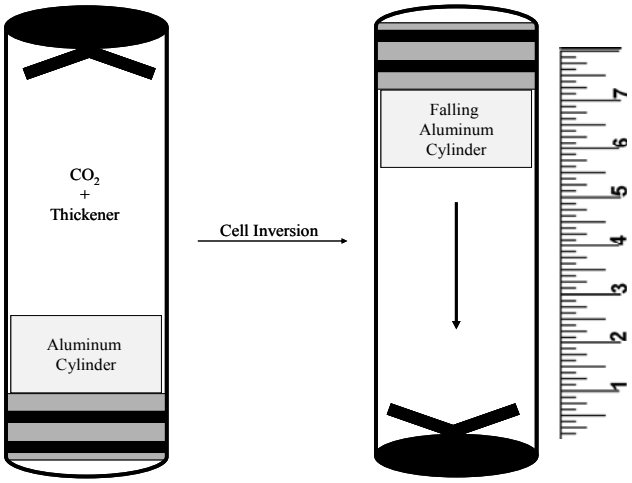

Figure 6. Illustration of falling cylinder viscometry

2.3 FOAM STABILITY APPARATUS

The main objective of the foam stability apparatus is to determine whether a potential foaming surfactant with excellent solubility behavior in CO_2 is capable of forming stable foams with brine and CO_2 under specific reservoir condition. This is a further, more realistic investigation to

evaluate surfactants' feasibility in real industrial application. Most of our tests require super low concentration of a surfactant, mostly range within 0.03~1wt%.

At the beginning, a certain sample is placed on top of the piston, inside the glass cylinder, and the calculated amount of brine, according to the weight of the sample, is poured into the glass cylinder. Then the Robinson cell is tightly sealed. CO_2, with equal volume of brine, is introduced at 1600pisa, room temperature (~24^o C). The interface position, which separates the CO_2 and brine, is recorded. Then, the system is kept mixing until the glass cylinder is filled up with cloudy, steady foams. Once the magnetic stir is stopped, the data collection starts in terms of time. The foam would collapse toward the interface from the top and the bottom, and the lengths of foam left in both CO_2 and brine phase are collected. After an experiment, two curves showing the foam stability are generated based on those data points. The following graph shows the whole process of a foam stability test, for an excellent surfactant.

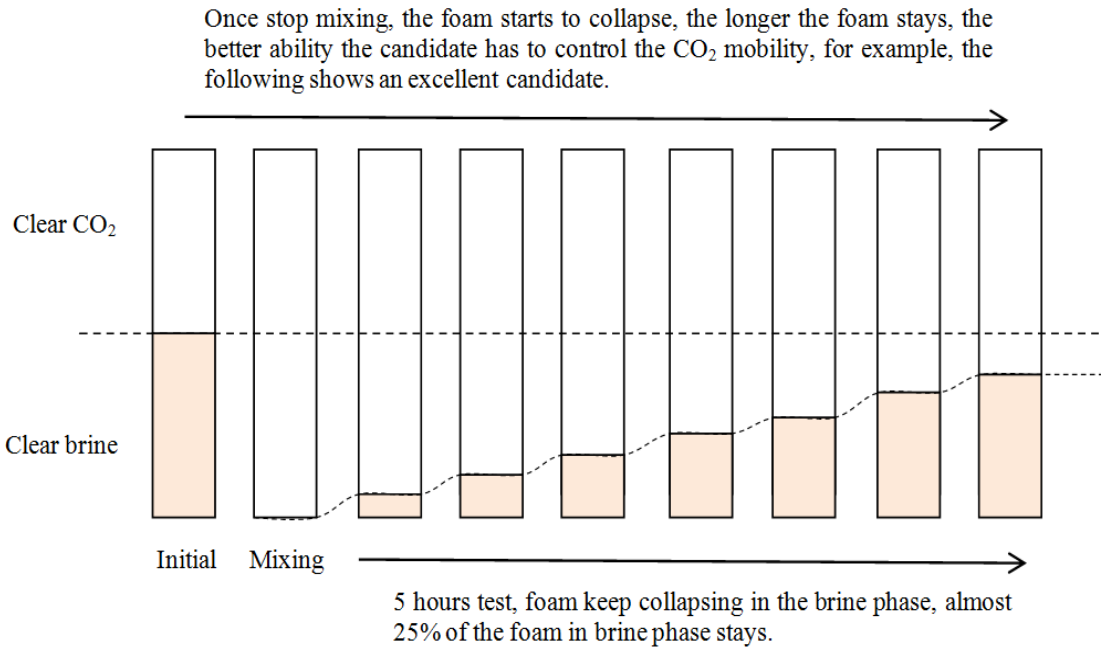

Figure 7. Illustration of foam forming and collapsing

2.4 CO_2 MOBILITY TEST UNIT

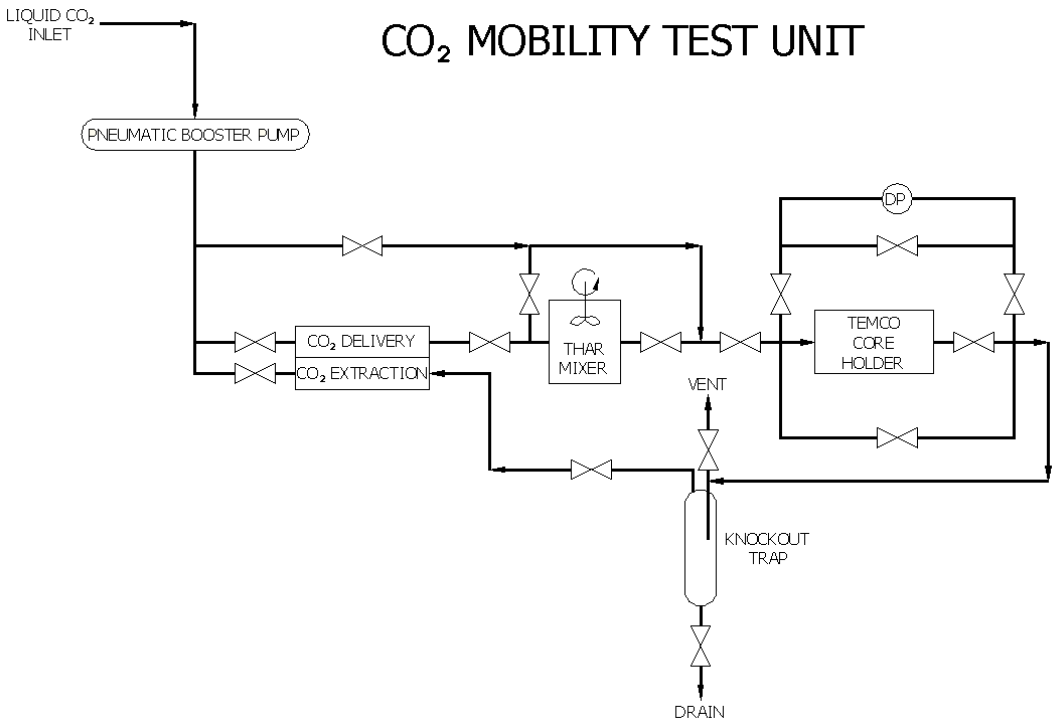

Figure 8. CO_2 flooding through porous media apparatus

The objective of the experiment is to displace a single phase CO_2 solution through the sandstone core at a constant flow rate. The pressure of thickened CO_2 is maintained at a higher pressure then different cloud point pressure, in order to ensure a homogeneous single phase flow. The candidate is placed in the reactor at the very beginning, and then the whole system is flooded by CO_2. Water is introduced into the core holder as the overburden fluid, typically 500psi higher than the system pressure. The reactor is isolated and stirred until a single homogeneous phase is observed through the window. The thickened CO_2 in the reactor is then pushed into sandstone by a positive displacement pump as the equal volume of CO_2 is expanded at the same volumetric rate in the reversal displacement pump. And three pressure differentials are collected along the

sandstone core. Fluid viscosity can be determined with Darcy's law for the flow of a Newtonian fluid through porous media in the creeping flow regime.

The pressure drops through the core are monitored continuously as the CO_2 solution flows through the core at a superficial velocity of 1 or 10ft/day, typical flow rates in oil field. There are three pressure transducers, which collect the pressure drops along each third of the core. Such design facilitates the detection of candidates' retention at the entrance of the core (the first third of the core), which would exhibit a much higher pressure drop than that in the rest of the core.

3.0 RESULTS OF DIRECT THICKENERS

The key to directly enhance the viscosity of CO_2 under typical reservoir condition is to discover or design a high molecular weight thickener soluble in CO_2 at sufficient concentration and capable of thickening CO_2 without using any other co-solvent. Previous results related to direct thickeners shows that only polyFAST (fluoroacrylate-styrene copolymer, 29% styrene and 71%fluoroacrylate monomer) exhibits the most significant viscosity enhancement. Without using these CO_2-philic, expensive, fluorinated functional groups, the thickeners primarily consist of carbon, hydrogen and oxygen are either insoluble in CO_2 even at 10000psi or incapable of giving evident CO_2 viscosity enhancement. Therefore, associative macro-networks, like non covalent interaction, hydrogen bonding and π-π stacking by aromatic groups or charge transfer forming the "glue" that holds the system together [27], gain our most recent interest for direct thickener project.

The basic idea is to have CO_2-philic groups incorporated in the thickener structure to improve solubility, and also have the macro-interaction among the solute molecules to form large network through the abovementioned theories. However, CO_2, a weak solvent for polar and high molecular weight compounds, usually could not dissolve efficacious amounts of these direct thickeners under traditional reservoir conditions, even though they successfully gelled other types of solvent. The priority lies on the augmentation of direct thickeners' solubility in CO_2. We

have tried several candidates with highly branched hydrocarbon tails connected to different metal moieties, the results are discussed in the following section.

3.1 SELF-ASSEMBLY FLUORINATED DI-CHAIN SURFACTANTS

Although the objective of this research remains the design of non-fluorinated, small, CO_2 thickening agents, self-assembly fluorinated di-chain surfactants represent the first example of CO_2 viscosity modifiers based on anisotropic reversed micelles, since water is not included in the previous system like polyFAST and other small molecules thickener. These type of surfactants are capable of enhance CO_2 viscosity through self-aggregation and forming cylindrical rod-like micelles. And the best candidate of this type thickener can lead to viscosity enhancements of up to 90% compared to pure CO_2 at 10wt%.

A commonly studied surfactant in organic media is Aerosol—OT (AOT, sodium bis-2-ethylhexyl sulfosuccinate, also known as docusate sodium), since di-alkyl sulfosuccinate moiety represents a flexible tail for designing new surfactants for various reverse micelles formation [28-32]. For our research, the di-alkyl sulfosuccinate surfactants have been modified to prepare CO_2-soluble surfactants that form viscosity-enhancing rod-like reversed micelles. Firstly, exchange of the Na^+ counterion for Co^{2+}or Ni^{2+} has been employed to achieve divalent surfactants. For normal AOT-stabilised microemulsions in organic solvents, such as cyclohexane, exchange of Na^+ for Co^{2+} or Ni^{2+} is known to drive a sphere-to-rod transition, promoting viscosity enhancements up to 40-fold at 10wt% surfactant [33-35] supported by the small-angle neutron scattering (SANS) data from Dr. Julian Eastoe's research group. Secondly, normal AOT is itself essentially insoluble in CO_2 [36], so Co^{2+} and Ni^{2+} surfactants are rendered

CO_2 soluble by substitution of hydrocarbon for fluorocarbon chains, to generate bis(1H,1H,5H octafluoro-n-pentyl) sulfosuccinate (di-HCF4) surfactants. Such fluorinated di-chain AOT-analogues are known to stabilize reversed water-in-CO_2 (w/c) microemulsions; [37-39] The custom-made Na(di-HCF4), Co(di-HCF4)$_2$ and Ni(di-HCF4)$_2$ surfactants are shown below:

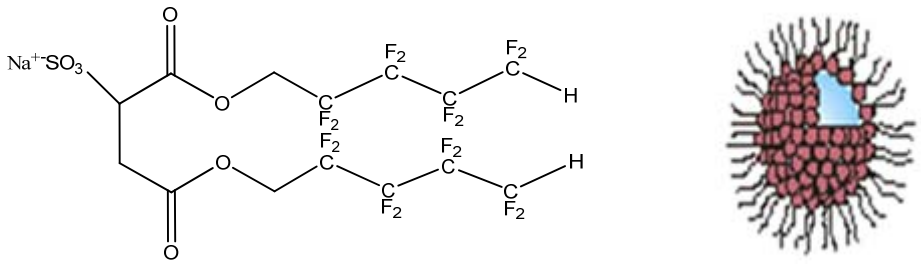

Figure 9. Structure of fluorinated monovalent surfactant, Na(di-HCF4)

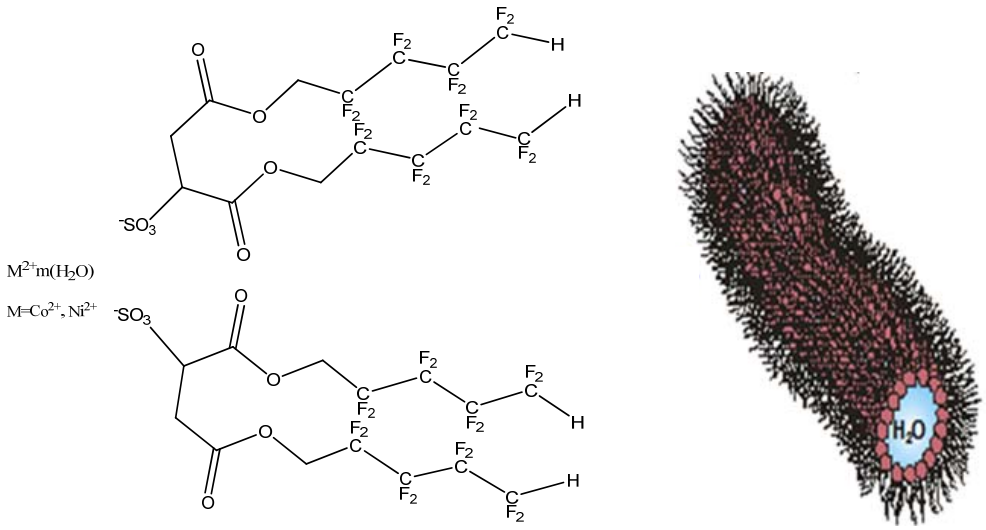

Figure 10. Structure of fluorinated divalent surfactants,Co(di-HCF4)$_2$ and Ni(di-HCF4)$_2$

Such fluorinated di-chain AOT-analogues are known to stabilize reversed water-in-CO_2 (w/c) microemulsions; in particular di-HCF_4 is recognized to be an effective and relatively inexpensive compound. This study demonstrates that the two basic principles of designing CO_2 thickeners, which can be applied to achieve control over aggregation, and as a result, significant viscosity enhancements in CO_2.

3.1.1 Phase behavior results of fluorinated Co, Ni, di-chain surfactants

W represents the water/surfactant molar ratio, and V-L-L line means the liquid-liquid-vapor points. Fluorinated sodium surfactant is our baseline for comparison in these three surfactants, shown in Figure 11, and the red data point is attained from Dr. Eastoe's research group, which is a repeat phase behavior experiment in different apparatus.

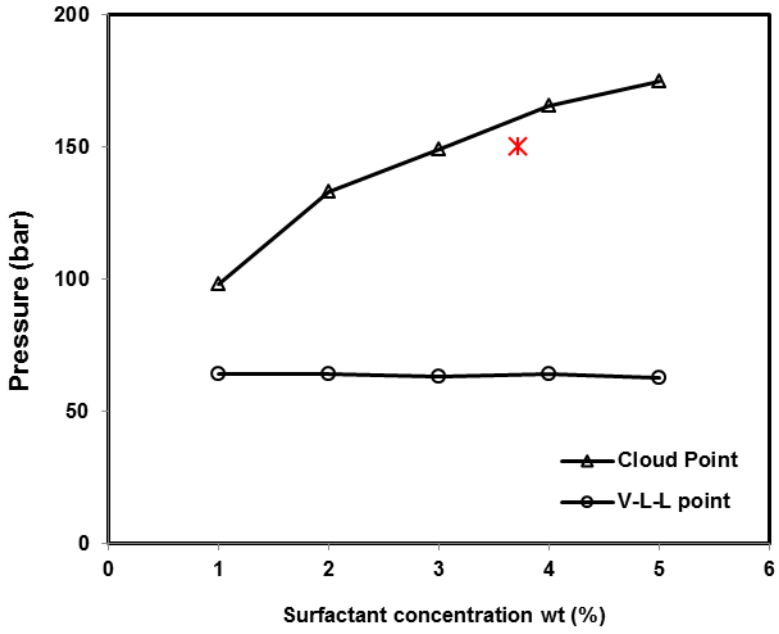

Figure 11. Phase behavior result of fluorinated sodium surfactant, w=0, T=25°C

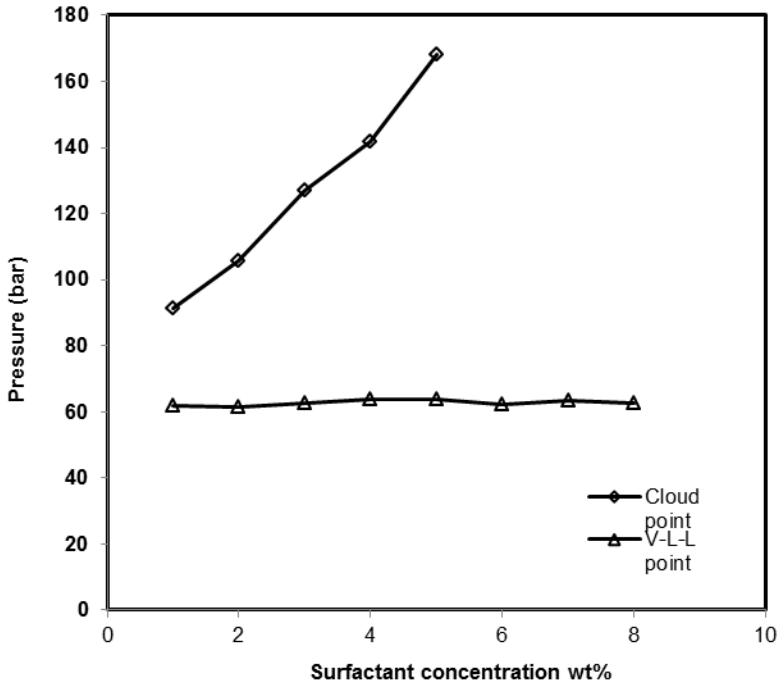

Figure 12. Phase behavior of fluorinated nickel surfactant, w=0, T=25°C

Water is necessary for forming micelles, therefore we also run phase behavior experiment specifically on $Co(di\text{-}HCF4)_2$ to find out the effect of water introduction to the system, shown in Figure 13. W represents the water (added)/CO_2 molar ratio, with the increase of w, it becomes more difficult to dissolve the same concentration of surfactants in CO_2. As a result, minimum water addition is necessary, which is just above the CMC (critical micelle concentration).

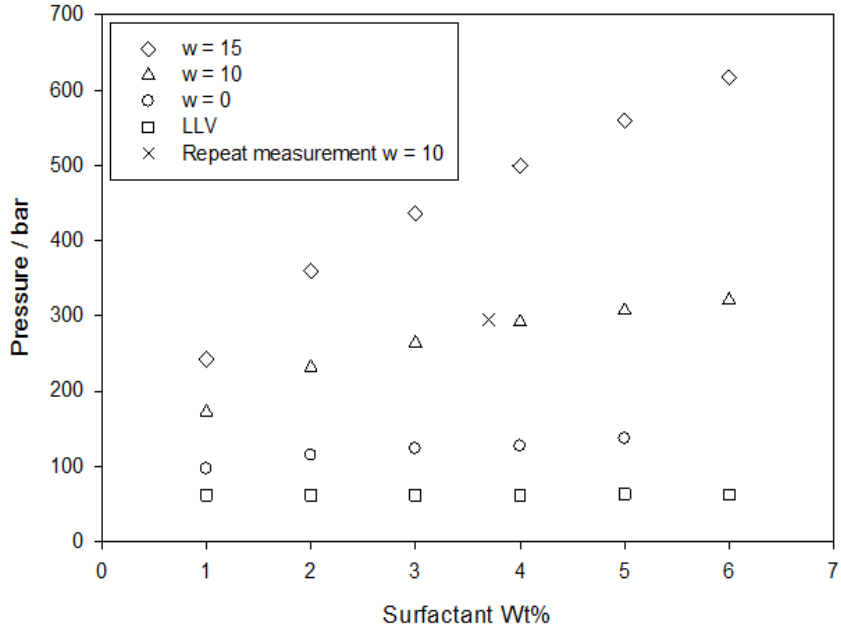

Figure 13. Phase diagram comparing effect of surfactant concentration and W on the stability of Co(di-HCF4)$_2$ surfactant in CO_2 at 25 °C. Point marked x represents a repeat conducted, with the same surfactant batch, but in a different cell and by a different operator

3.1.2 Viscosity enhancement results of Self-assembly fluorinated di-chain surfactants

High-pressure viscosity measurements at 25^{o}C and 350 bar are reported in terms of η_{mic}/η_{CO2}, the ratio of microemulsion viscosity (η_{mic}) compared to that for neat CO_2 (η_{CO2}), as determined from data for the ratio of the terminal velocity of the cylinder falling through neat CO_2 to that for the microemulsion. With Na(di-HCF4) only modest viscosity enhancements were noted: for example at 6wt% η_{mic}/η_{CO2} signifies merely a 15% increase in viscosity over CO_2 alone. This is consistent with expectations based on the SANS data and analyses, because dilute spherical droplets formed by Na(di-HCF4) should result in only minimal effects on η_{mic}.(all the SANS results and conclusions are from Dr.Eastoe's research group)

On the other hand, as shown in Figure 14 for the rod micelle forming Ni(di-HCF4)$_2$, a distinct viscosity increase was observed at 6 wt% with $\eta_{mic}/\eta_{CO2} \sim 1.4$ (~ 40% greater than CO_2). Notably, as surfactant concentration was increased up to 10 wt% the ratio η_{mic}/η_{CO2} nearly doubles. Viscosities for the Co(di-HCF4)$_2$ surfactant were also determined, as for the Ni^{2+} derivative this Co^{2+} surfactant exerts a greater effect on viscosity compared to the Na^+ analogue, and $\eta_{mic}/\eta_{CO2} \sim 1.2$ at 6 wt%, raising to 1.6 (i.e. 60%) at 7 wt% of Co(di-HCF4)$_2$.

The range of the shear rates for these experiments varied between 6000 – 11000 s^{-1} at the surface of the falling cylinder; the Reynolds number values were 25 – 92. For example, for a 10wt% solution of Ni(diHCF4)$_2$ in CO_2 at 25^{o}C, 350 bar and w = 10 the rotational Peclet number has a value of 0.002. This value is low despite relatively high shear rates because of the small size of the micelles and the low viscosity of dense CO_2, therefore Brownian forces dominate and the micelles are likely to be nearly randomly oriented. Consequently, one would not expect significant increases in viscosity at lower shear rates, including the 10–100 s^{-1} range encountered during CO_2 floods in sandstone or limestone oil reservoirs. Unfortunately, we did not have enough surfactant samples to perform a series of viscosity experiments at each concentration using cylinders of varying diameter, which would have provided quantitative experimental evidence of shear-thinning over a broad range of shear rates. Nonetheless, the results obtained in this work indicate that the viscosity-enhancing ability of these surfactants is comparable to that of tri(semifluorinatedalkyl)tin fluorides and fluorinated telechelic ionomers assessed over a comparable range of shear rates [40], but less than that of random copolymers of fluoroacrylate and styrene [41-43].

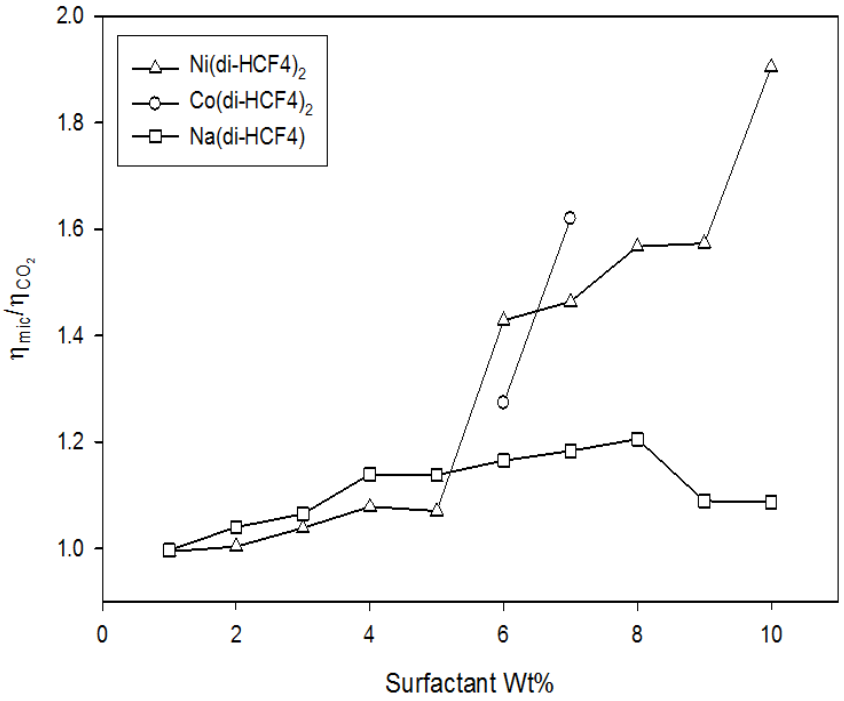

Figure 14. High-pressure viscosity measurements at 25°C, 350 bar and w = 10 showing the effect of surfactant counterion on relative viscosity η_{mic}/η_{CO2}, the ratio of microemulsion viscosity (η_{mic}) compared to that for neat CO_2 (η_{CO2})

3.2 ALUMINUM DI-SOAPS

The general structure of aluminum di-soaps is shown below:

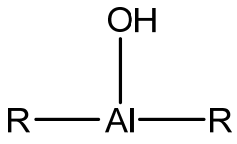

Figure 15. General structures of aluminum di-soaps

The two R groups are designed to increase the solubility of the compound in CO_2 while promoting the formation of viscosity-enhancing macromolecules via the hydroxyl groups

interacting with the aluminum of the neighboring molecule hydrogen bonding. There are several of these aluminum disoaps, such as hydroxyaluminum di(2-ethyl hexanoate), with an excellent ability to thicken hydrocarbons such as hexane and toluene at concentrations as low as ~0.1wt%. For our research, we try to utilize these surfactants to thicken CO_2 without a co-solvent. Because AlOH bis-2-ethyl-hexanoic acid is not soluble in CO_2, more CO_2-philic R groups will be selected. Even if the compound dissolves in CO_2, it will not ensure that viscosity enhancement will occur. The relationship between the thickening potential of an R group and the structure of the R group remains primarily empirical at this point; for example while both AlOH(2-ethyl hexanoate)$_2$ and AlOH (octanoate)$_2$ are hexane soluble, only AlOH(2-ethyl hexanoate)$_2$ induces a tremendous viscosity enhancement.

3.2.1 Synthesis of aluminum di-soaps

The surfactants were prepared using the procedure stated by U.S.Patent 2741629. Generally, a certain carboxylic acid with the specific hydrocarbon tail reacts with excessive amount of sodium hydroxide and aluminum sulfate octodecahydrate to prepare aluminum di-soaps. Specifically, sodium hydroxide is usually in excess of 1.5: 1 of carboxylic acid and aluminum sulfate is usually in an excess of 1.2:1 of carboxylic acid. We have synthesized the following aluminum di-soaps with different CO_2-philic hydrocarbon tails.

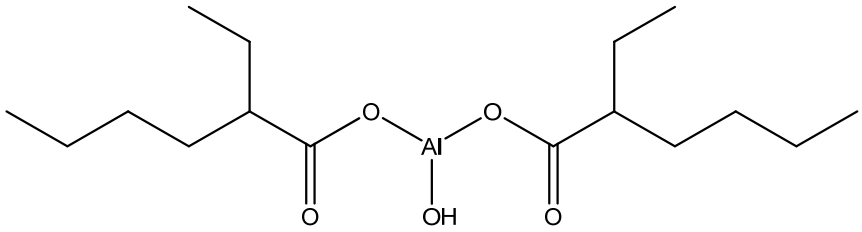

Figure 16. Structure of hydroxyaluminum di-2-ethyl-hexanoic tail soap

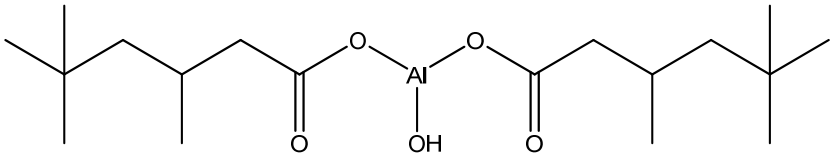

Figure 17. Structure of hydroxyaluminum di-3,5,5-trimethyl hexanoic tail soap

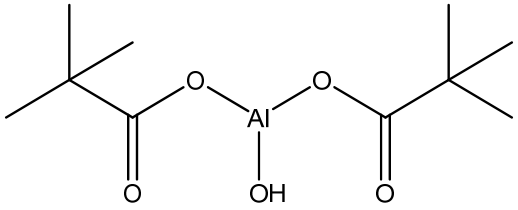

Figure 18. Structure of hydroxyaluminum di-pivilic tail soap

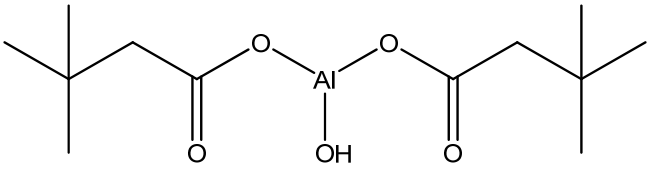

Figure 19. Structure of hydroxyaluminum di-terbutyl acetic tail soap

The synthesis procedures of the hydroxyaluminum di-2-ethyl-hexanoic tail soap is shown below, and the synthesis of hydroxyaluminum di-3,5,5-trimethyl hexanoic tail soap, hydroxyaluminum di-pivilic tail soap and hydroxyaluminum di-terbutyl acetic tail soap follows the same procedure.

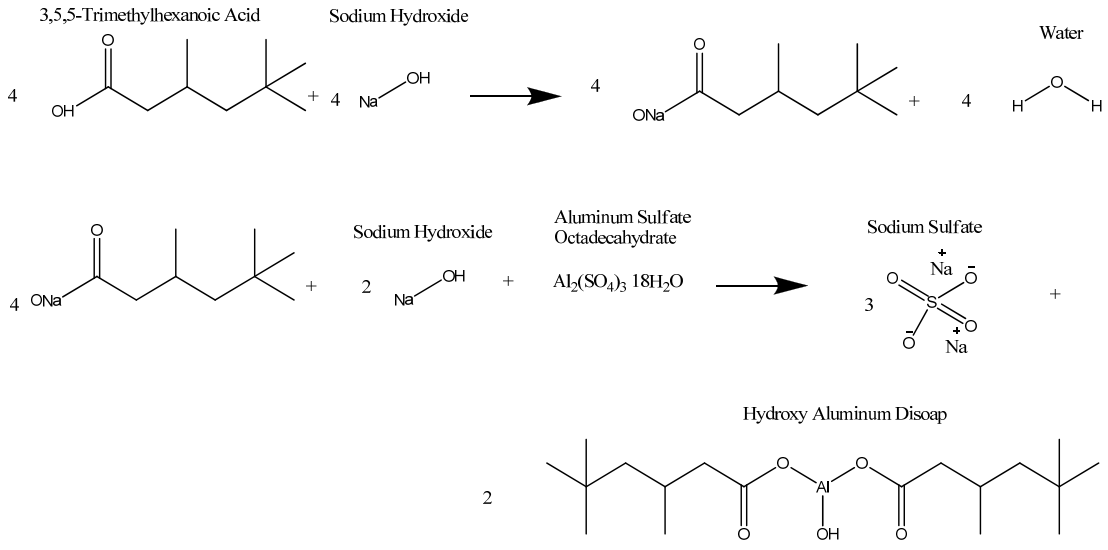

Figure 20. General synthesis procedures of aluminum di-soaps

3.7 grams of sodium hydroxide pellets were combined with 72 mL of water in an Erlenmeyer flask at room temperature on mixing plate for 5 minutes. 9.49 mL of 2-ethylhexanoic acid liquid was added to this beaker at room temperature. The solution was stirred until at room temperature. 10.15 grams of aluminum sulfate octadecahydrate powder was dissolved in 25 mL of water, needed to be stirred at room temperature for 10 minutes. This dissolved solution was added in a slow stream to the reaction vessel containing the cooled sodium hydroxide and 2-ethylhexanoic acid mixture. After the reaction was completed, about 20 minutes, the product was extracted using filtration. The product was washed until no sulfate ion was present. This can be tested by using the barium chloride test where saturated barium chloride is added to the filtrate, if no precipitate results then there is no more sulfate ion in the product. Usually the product needed to be washed by 20 mL of water six times. After the product is filtered, the product will need to be dried for at least 24 hours. The product needs only

to be at room temperature to dry. After drying the usual product yield for (2-ethylhexanoic acid)$_2$·AlOH is 90 %.

3.2.2 Solubility results of aluminum di-soaps in hexane

Before these aluminum disoaps are put into the Robinson cell, we test their ability of thickening hexane. And the following table shows the results:

Table 1. Solubility results of aluminum di-soaps in hexane

Surfactant	Wt%	Visibly Thickens Hexane?
(2-ethylhexanoic acid)$_2$· AlOH	0.1	No
	0.2	No
	0.5	Yes, cloudy thickened liquid
	1.0	Yes, cloudy blob
	1.5	Yes, cloudy blob
	10	Yes, cloudy blob
(3,5,5-trimethylhexanoic acid) $_2$· AlOH	0.1	No
	0.2	No
	0.5	No
	1.0	No
	1.5	No
(Pivalic acid) $_2$· AlOH	0.5	No
	1.0	No
	1.5	No
(tertbutyl acetic acid) $_2$· AlOH	0.5	No
	1.0	No
	1.5	No

But unfortunately, even at the lower concentration condition, these aluminum disoaps are not able to dissolve in CO_2 at around 9300psi. Therefore, there is no viscosity enhancement test on these aluminum di-soaps. Apparently the hydroxyaluminum head is strong CO_2-phobic, even with excellent CO_2-philic tail incorporated.

Table 2. Solubility results of aluminum di-soaps in CO_2

Surfactant	Lowest Wt% In co2	Visably dissolved in CO_2 ?
(2-ethylhexanoic acid)$_2$· AlOH	0.3	No, T = 25°C P = 9000 psi
(3,5,5-trimethylhexanoic acid) $_2$· AlOH	0.05	No, T = 50°C P = 9000 psi
10 weight % of (2-ethylhexanoic acid)$_2$· AlOH in 25 mL of Hexane (mixing surfactant and hexane)	0.5	No, T = 25°C P = 9355 psi
(Pivalic acid) $_2$· AlOH	0.1	No, T = 25°C P = 9300 psi

We also tested another two aluminum di-soaps synthesized by Dr. Eastoe's research group, their structures are shown below:

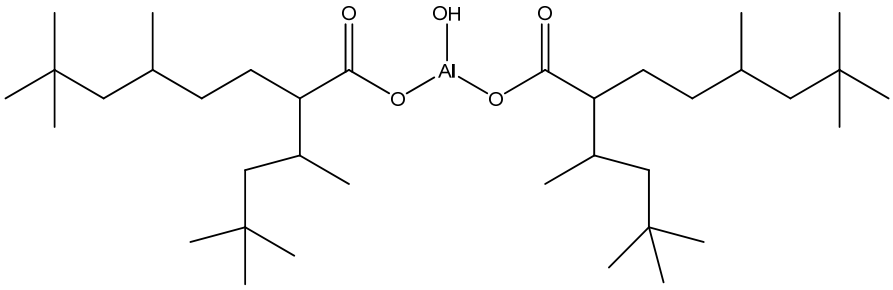

Figure 21. Structure of hydroxyaluminum di-isostearate-N soap

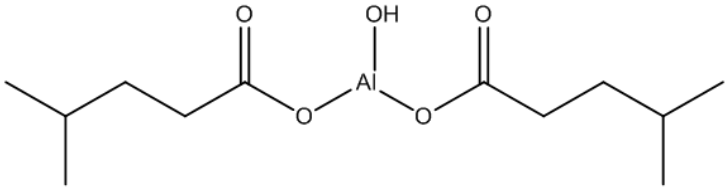

Figure 22. Structure of hydroxyaluminium di-(4-methylvalerate) soap

Unfortunately, neither of these aluminum disoaps showed solubility in CO_2 under our lab condition.

3.3 VISCOSITY RESULTS FOR 2-ETHYL-HEXANOIC ACID

2-ethyl-hexanoic acid has decent solubility in CO_2 solution, and it is observed in Robinson Cell for its viscosity enhancement ability. Under 5000psi and room temperature, there is no distinct viscosity enhancement by adding 2-ethyl-hexanoic acid into liquid CO_2.

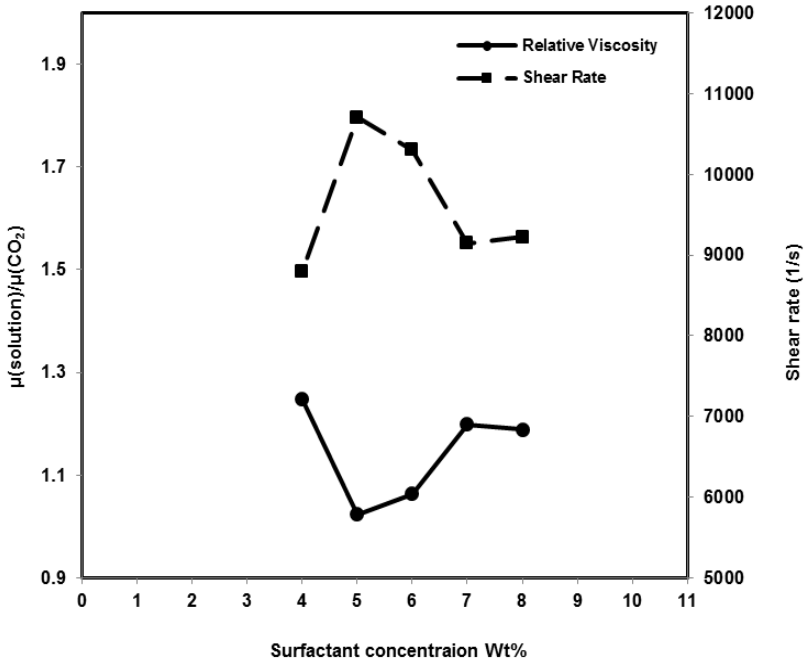

Figure 23. High-pressure viscosity measurements for 2-ethyl-hexanoic acid at 25°C, 5000psi

4.0 RESULTS OF FOAMING AGENTS

The objective of the current research is to identify or design inexpensive surfactants that are sufficiently soluble in CO_2 to readily dissolve in the CO_2 being injected into a reservoir and then generate CO_2-in-brine foams. These surfactants could then be used to enhance mobility control or to block off highly permeable watered-out zones via the WAGS process or in the simple injection of a CO_2-surfactant solution into a reservoir. The desirable attributes of the surfactant included.

1. *Efficacious at MMP* – much progress has been made in the design of surfactants that dissolve in CO_2 at very high pressures (e.g. 3000-20,000 psi at ambient temperature). The surfactants used in this oilfield application, however, must be soluble in CO_2 at typical surface conditions where the surfactant would be added to the CO_2, and within the reservoir at reservoir temperature and typical MMP values. For example, at 25^{o}C, MMP values as estimated by numerous MMP correlations are in the 1000-1500psi range.

2. *Non-ionic* – Although several research groups, including our own, have generated numerous CO_2-soluble ionic surfactants, the pressure required to dissolve even small amounts of these surfactants is typically greatly in excess of typical MMP values. Unlike water, the solvent strength of CO_2 simply is not greatly enough to solubilize ionic surfactants at typical EOR pressures.

3. *Non-fluorous* – It is well known that the CO_2-philicity of the surfactant tails can be greatly enhanced via the addition of highly fluorinated tails (e.g. fluoroethers, fluoroacrylates). Such functional groups are usually quite expensive however, and do not lend themselves to the design of a practical oilfield surfactant.

4. *CO_2-philic hydrocarbon tails* – The CO_2-philic tail(s) of the surfactant should be based on hydrocarbons, if possible. Therefore this work has assessed (a) linear alkyl chains, (b) branched alkyl chains, (c) linear alkylphenol chains, and (d) branched alkylphenol chains. Hydrocarbon tails lacking the phenol group (i.e. benzene ring) are likely to be more environmentally benign than the alkylphenol ethoxylates (e.g. nonylphenol ethoxylates) with regard to degradation products.

5. *Avoid expensive hydrocarbon-based CO_2-philes* – There are several oxygenated hydrocarbon-based tails that are also very CO_2-philic, including oligoVAc, oligo lactic acid, sugar acetates, and (to a much lesser extent) oligo butylene glycol. Although these CO_2-philic segments may be promising for the scientific development of foaming surfactants, such surfactants are not commercially available in large amounts at the current time and would likely be very expensive if generated in large amounts using current synthetic methods, with the possible exception of BO-EO surfactants.

6. *Ethylene oxide hydrophiles* – Oligomers of ethylene glycol will be used. This is the most commonly available and inexpensive nonionic hydrophile that is currently available.

7. *Water soluble, rather than water-dispersible or water-immiscible* – Based on Bancroft's rule, the surfactant should be more soluble in the continuous, low volume, aqueous phase than in the high volume, discontinuous, dense CO_2 phase. Although the surfactant needs to be slightly CO_2-soluble in order to dissolve in the CO_2 being injected into the reservoir, it should be so water-soluble that it will partition into the brine phase within the porous media, allowing surfactant-stabilized lamellae to form within the sandstone or limestone pores.

8. *Not too water soluble*- If one continues to extend the PEG tail of these non-ionic surfactants too far, the surfactant will become CO_2-insoluble due to its high molecular weight. Therefore it is likely that an optimal range of EO groups will occur; if there are too few EO groups the surfactant will be water-insoluble and unable to stabilize the desired emulsion or foam, but if the number of EO groups is too large the surfactant will become more water-soluble but its CO_2-solubility will diminish.

9. *Liquid surfactant* – The surfactant would be easier to handle, pump and mix with the dense CO_2 if it was a liquid, rather than a solid.

10. *Dilute concentrations* – CO_2 is a feeble solvent relative to water for the dissolution of surfactants. Therefore the concentration of surfactant to be dissolved in CO_2 is quite likely to be small, ~ 0.01 – 0.1wt% or 100 – 1000 ppm, relative to the concentration of surfactant that can dissolved in brine during the SAG process.

With the abovementioned rationale for the selection of foaming agents, all of the surfactants are hydrocarbon-based non-ionics that are commercially available in large quantities at prices in the $0.75 - $3/lb range. And we have 3 major categories of foaming agents, branched alkylphenol ethoxylates, linear alkyl ethoxylates and linear ethoxylates.

4.1 BRANCHED ALKYLPHENOL ETHOXYLATES

4.1.1 Sigma-Aldrich Triton X-100, Huntsman Surfonic OP 100, and BASF OP 10

They share the exactly same structure as shown below:

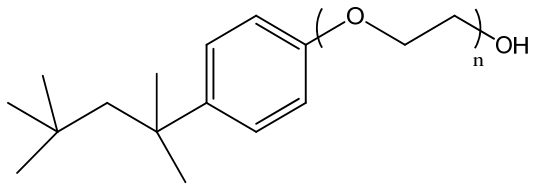

Figure 24. Structure of Sigma-Aldrich Triton X-100, Huntsman Surfonic OP 100, and BASF OP 10, n=9~10

4.1.1.1 Solubility results of Triton X-100, Huntsman Surfonic OP 100, and BASF OP 10

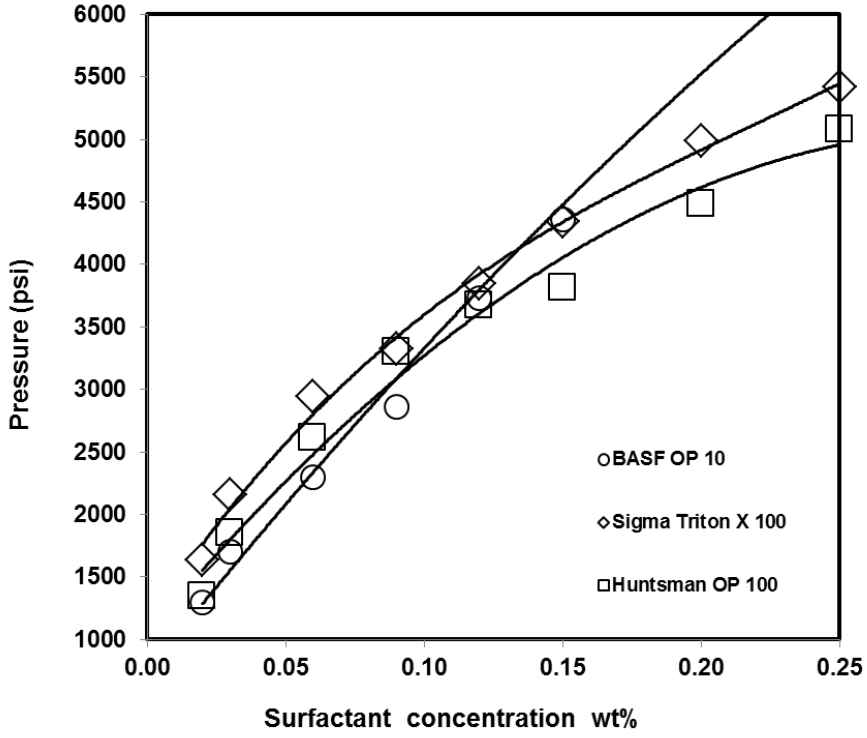

Figure 25. Solubility of Triton X-100, Huntsman OP 100 and BASF OP 10 in CO_2 at 25°C

The solubility of Dow Triton X 100, BASF Lutensol OP 10, and Huntsman octylphenol Surfonic OP 100 branched octylphenol ethoxylates at 25°C is the case with all of the surfactants investigated in this study, the cloud point pressure increases with concentration. At 25°C and 1000psi (~6.9MPa), the solubility of Triton X 100 is roughly 0.02wt%, far below the 1wt% value assumed by Bernard and Holm (Bernard 1967) [6]. The samples provided by three manufacturers exhibited similar solubility values at pressures below 4000psi (~27.7MPa).

4.1.1.2 Foam stability results of Triton X-100, Huntsman Surfonic OP 100 and BASF OP 10

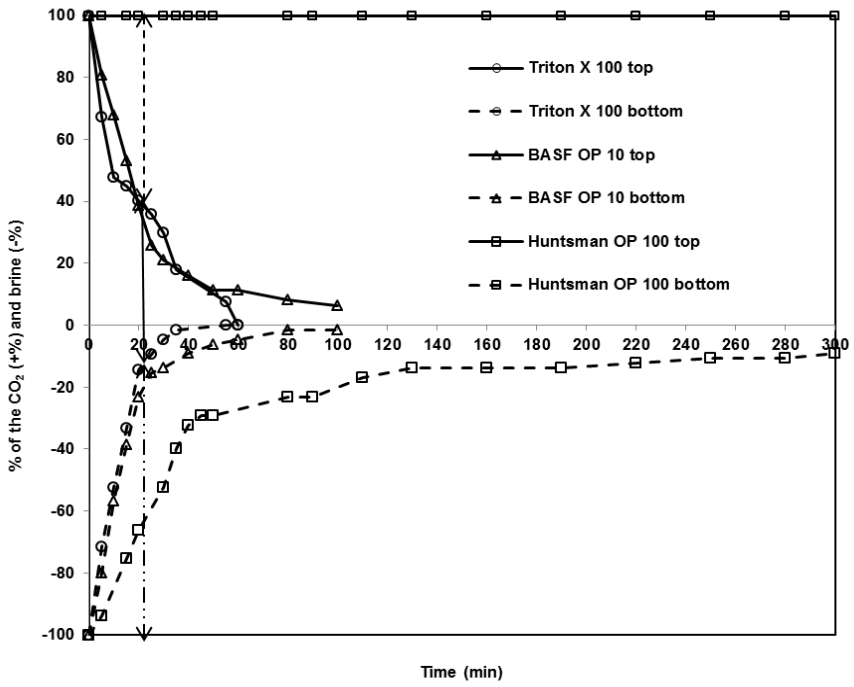

Figure 26. 0.04wt% Triton X-100, Huntsman OP 100, and BASF OP 10 in CO_2 at 1300psi and 25 ºC, with a brine (5wt%NaCI)/CO_2 volume ratio 1:1

The branched octylphenol ethoxylates obtained from three different manufacturers provided very similar foam stability results, Figure 26, when present in a concentration of 0.04wt% relative to the mass of CO_2. In the case of the third sample, Huntsman OP 100, the foam remained stable for five hours. At concentrations of 0.02wt% or less, this surfactant did not stabilize foams.

4.1.2 DOW Tergitol NP series

DOW Tergitol NP series includes NP-4, NP-6, NP-9, NP-12, and NP-15. They all have 9 branched carbons, the difference lies on their ethoxylate group number (4-15).

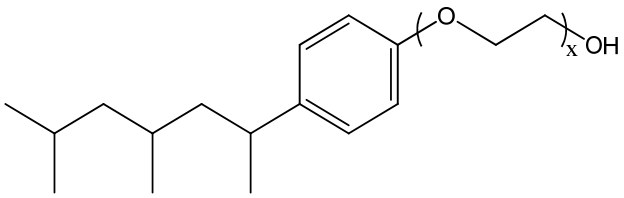

Figure 27. Structure of DOW NP Series, x = 4,6,9,12,15 (alkyl chain structure is proprietary; this is a qualitative representation)

4.1.2.1 Solubility results of DOW Tergitol NP series

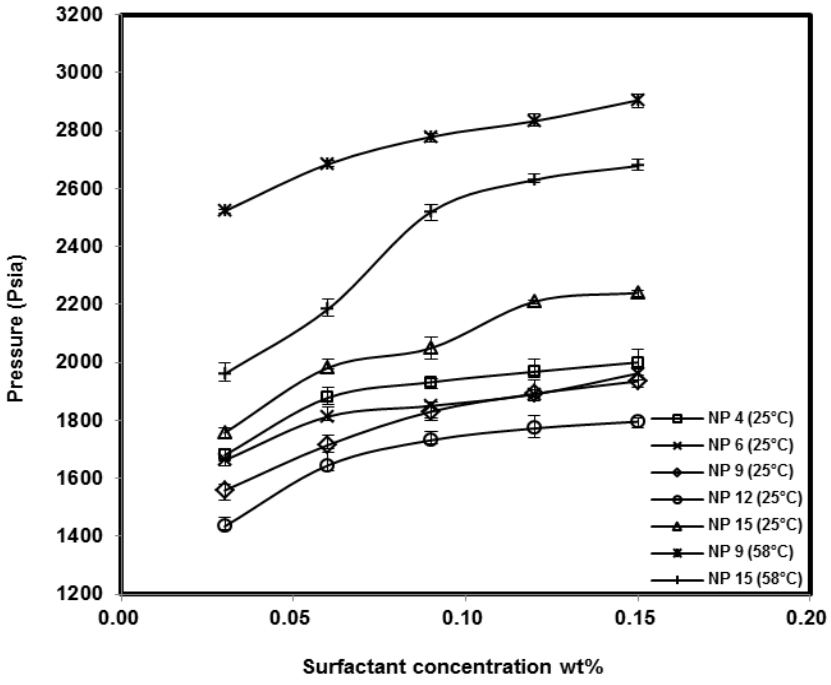

Figure 28. The solubility of NP series in CO_2 at 25ºC, also NP 9 and NP 15 at 58ºC

NP surfactants with 4, 6, 9, 12 and 15 EO repeat units were all found to be slightly soluble in CO_2. The branched nonylphenol group is hydrophobic and CO_2-philic, while the polyethylene glycol group is CO_2-philic and strongly hydrophilic. The most CO_2-phobic portion of the surfactant structure is the terminal hydroxyl group (-OH). As the length of the poly(ethylene glycol) increases from 4 to 6 to 9 to 12, the surfactant becomes more CO_2 soluble, as evidenced by a decrease in the cloud point pressure at a specified composition (i.e. the cloud point locus shifts to lower pressure). The results for the NP surfactants with 9 and 12 EO groups are comparable. Apparently, as the poly(ethylene glycol) from 4 to 12, the molecule becomes more CO_2-philic because the alkyl segment remains unchanged, the CO_2-philic PEG segment increases, and the CO_2 phobic hydroxyl group remains unchanged. As the PEG increases from 9 to 12 EO groups, however, the surfactant becomes more CO_2-philic and more hydrophilic (NP4 and 6 are not water soluble, but NP 9, 12 and 15 are water soluble), but the increasing molecular weight of the surfactant apparently has begun to diminish the CO_2 solubility of the surfactant. It is likely that the cloud point pressure will continue to increase as the length of the PEG segment increases beyond 12 EO groups. Note that at 25^{o}C and 1300 psi (a typical MMP at 25^{o}C), both NP 9 and NP 12 are about 0.04wt% soluble in CO_2.

4.1.2.2 Foam stability results of DOW Tergitol NP series

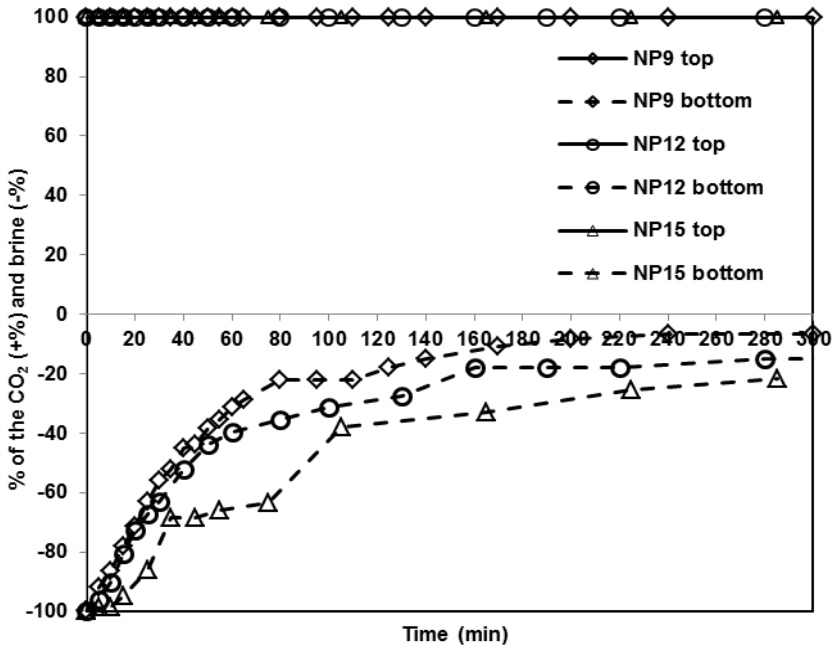

Figure 29. 0.04wt% NP9, 0.03wt% NP12 and NP15 surfactants in CO_2 at 1300psi and 25ºC, with a brine(5wt%NaCI)/CO_2 volume ratio 1:1

Neither NP4 nor NP6 is water-soluble, and neither was capable of stabilizing CO_2-in-brine emulsions at concentrations up to 0.02wt%. Excellent results were obtained with the NP9, 12 and 15 at 0.04wt%, 0.03wt% and 0.03wt%, respectively. In each case, a clear water zone gradually emerged but no clear zone of CO_2 appeared above the emulsion after 300 minutes. At 300 minutes, approximately 10vol%, 15vol% and 20vol% of the brine was retained within the emulsion along with all of the CO_2 for the NP 9, 12 and 15 surfactants. Therefore the emulsions for the NP9, 12, and 15 surfactants contained CO_2: brine volume ratios of 100:10, 100:15, and 100:20 after 300 minutes; or 9%, 13% and 17vol% brine emulsion quality, respectively.

4.1.3 Huntsman's Surfonic N series

Huntsman's Surfonic N85, N95, N100, N120, N150, N200, N300 and N400 are selected for experiments.

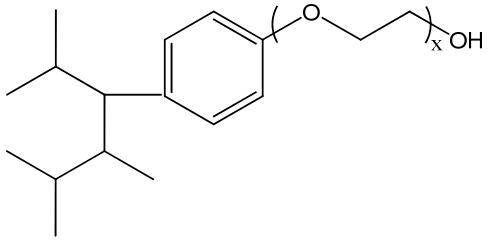

Figure 30. Structure of Huntsman Surfonic N series, x = 8.5, 9.5, 10, 12, 15, 20, 30, 40

4.1.3.1 Solubility results of Huntsman's Surfonic N series

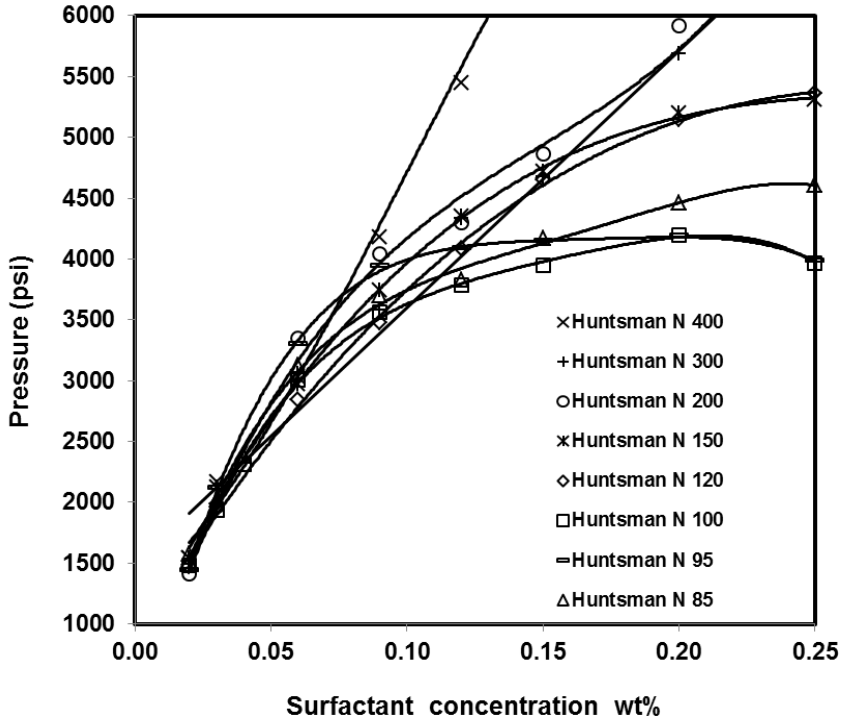

Figure 31. The solubility of Huntsman N series surfactants in CO_2 at 25 °C

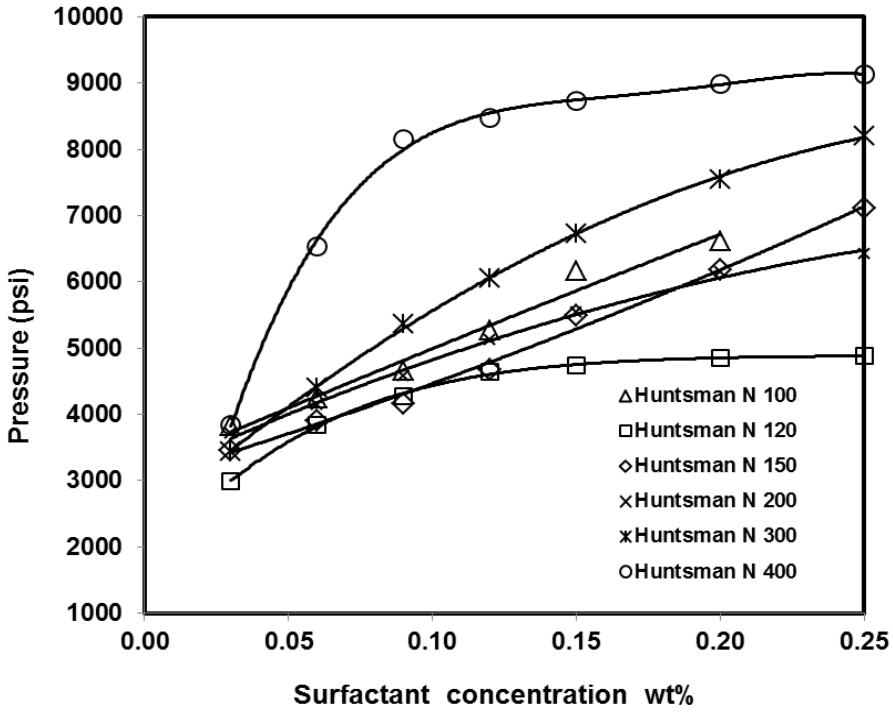

Figure 32. The solubility of Huntsman N series surfactants in CO_2 at 58 °C

The solubility values of the Huntsman branched, mixed isomeric, nonylphenol ethoxylates, Huntsman Surfonic N 85, 95, 100, 120, 150, 200, 300, and 400 at 25°C are presented in Figure 31. All of these surfactants are water-soluble, and the average number of EO groups corresponds to the surfactant designation divided by 10 (e.g. N120 has ~12 EO groups). The cloud point pressure of the surfactant increased with concentration and the solubility values of the Huntsman Surfonic N100 branched nonylphenol ethoxylate with 10 EO units was comparable to the solubility of the branched octylphenol ethoxylates with 10 EO units shown in Figure 25. The cloud point curves were comparable at concentrations less than 0.1wt%, but at higher concentrations the surfactants with the greatest number of EO groups (20–40) exhibited substantially high cloud point pressure values. The cloud point curves for the N12–N400 surfactants at 58°C are provided in Figure 32. The cloud point pressures have shifted to higher

pressures compared to the 25°C results, and the cloud point pressures at 58°C increase steadily as the number of EO groups in the hydrophile increases from 12 to 40.

4.1.3.2 Foam stability results of Huntsman's Surfonic N series

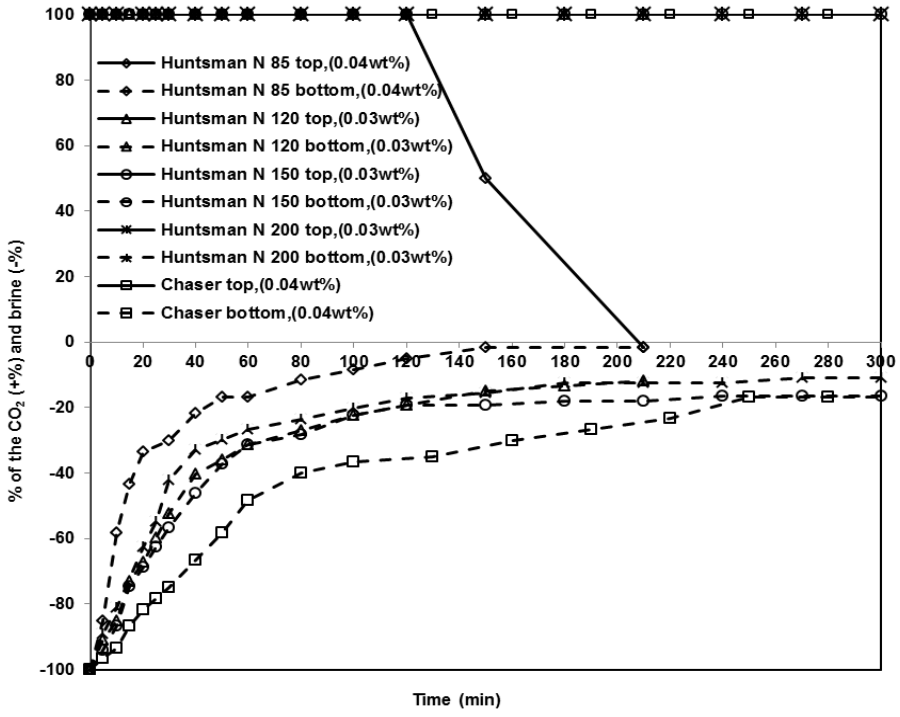

Figure 33. The foam stability associated with the Huntsman Surfonic N series foams at 1300psi and 25 °C, with a brine(5wt%NaCI)/CO_2 volume ratio 1:1; 0.04wt% N85, 0.03% N120 and N150, N200. Control results for water soluble Chaser CD 1045 at a concentration of 0.04wt% are also shown

Figure 33 illustrates the stability of the emulsions attained with the Huntsman Surfonic N surfactants. At 0.04wt% N85, the clear zone of brine began to form immediately, and the clear zone of CO_2 began to appear after 120 minutes. After 200 minutes, the emulsion had collapsed completely, leaving only clear zones of CO_2 and brine. Foams were also generated using the more water-soluble Huntsman N120, 150 and 200 at concentrations of 0.03wt%. The foams

were very stable; after 300 minutes, the CO_2-in-brine emulsion generated by Huntsman Surfonic N 120, 150 and 200 contained all of the CO_2 and ~20% of the brine, yielding an emulsion quality of 17vol% brine. The foams stabilized by 0.04wt% active CO_2-insoluble, water soluble Chaser CD 1045 were slightly more stable than any of the Huntsman Surfonic N surfactants. A comparison of Figures 26 and 33 indicates that despite the modest change in structure, the branched nonylphenol ethoxylates, which have one more carbon and mixed isomeric alkyl tails, provided superior foam stability relative to the branched octylphenol ethoxylates, which have only one C_8 alkyl structure.

4.1.4 Other branched alkylphenol ethoxylates

4.1.4.1 Structures of other branched alkylphenol ethoxylates

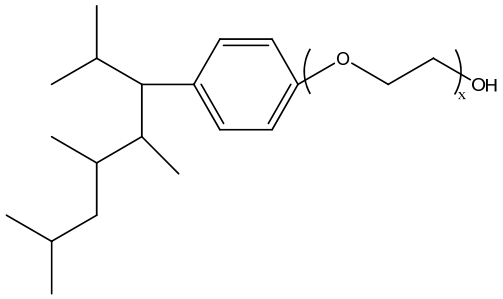

Figure 34. Structures of huntsman Surfonic DDP 100 (x = 10) and 120 (x = 12)

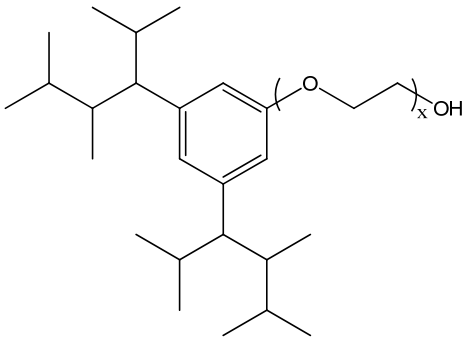

Figure 35. Structures of huntsman Surfonic dinonylphenol DNP 150 (x = 15) and 180 (x = 18)

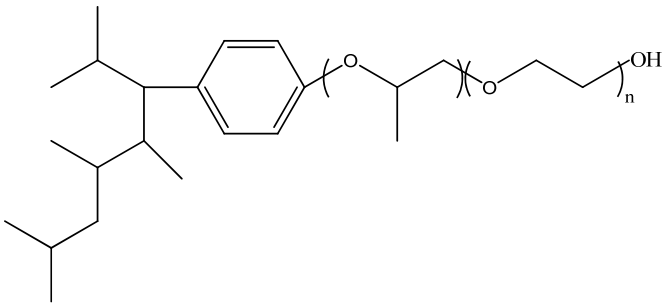

Figure 36. Structure of huntsman Surfonic N (PO1) 100 (n=10)

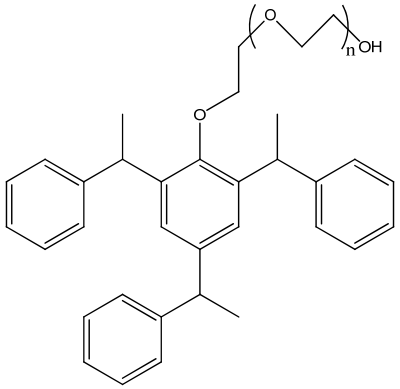

Figure 37. Structure of huntsman TSP 15, tristyrylphenol ethoxylates (n=15)

Stepan Cedepal CO 630 and 710, x = 10 and 10.5 share the same structure as Huntsman Surfonic N series shown in Figure 30.

4.1.4.2 Solubility results of other branched alkylphenol ethoxylates

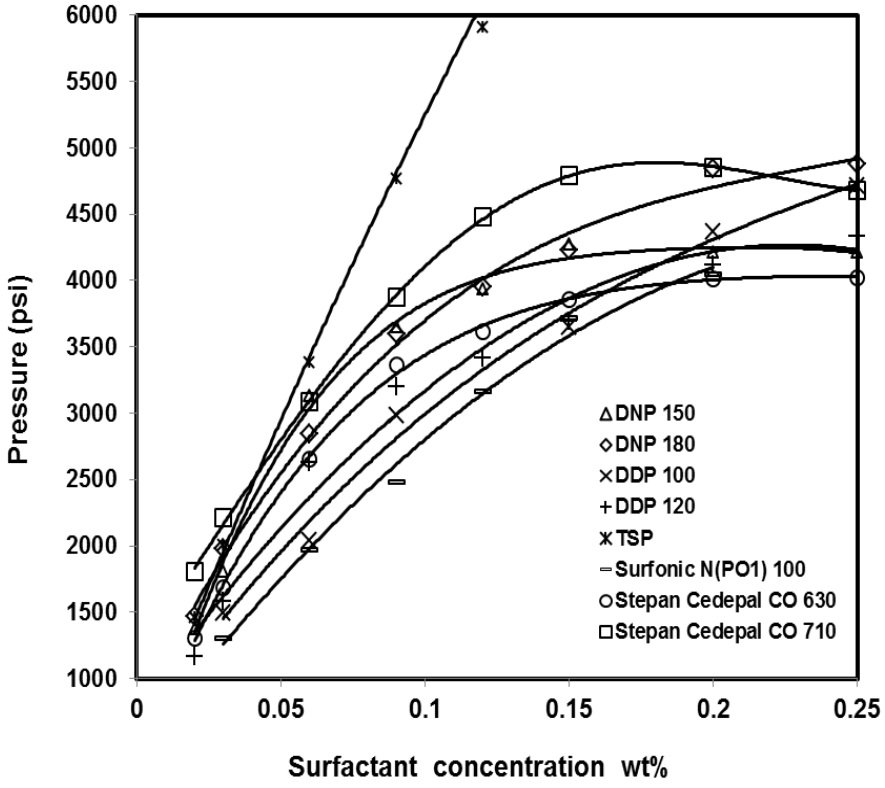

Figure 38. The solubility of Huntsman DNP150, 180, DDP 100, 120, TSP, Surfonic N(PO1) 100, Stepan Cedepal CO 630 and CO 710 in CO_2 at 25ºC

The solubility results of other branched alkylphenol surfactants are illustrated in Figure 38. In summary, the CO_2-solubility of the water-soluble, highly branched alkylphenol surfactants selected for this study are comparable in magnitude when compared on a weight percentage basis. Notably higher cloud point pressure values are exhibited for surfactants with ~30–40 EO units at concentrations greater than ~0.1wt%. The surfactants are roughly 0.02–0.05wt% soluble in CO_2 in the 1300–2000psi (~9–13.8MPa) range at 25°C, and in the 3000–3500psi (~20.7 – 24.1MPa) range at 58°C.

4.1.4.3 Foam stability results of other branched alkylphenol ethoxylates

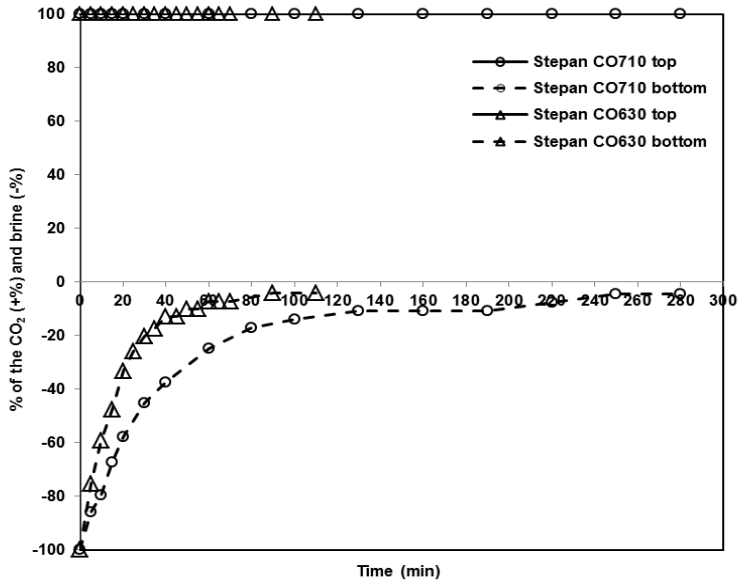

Figure 39. 0.03wt% Stepan CO 710 and CO 630 in CO_2 at 1300psi and 25ºC, with a brine (5wt%NaCl)/CO_2 volume ratio 1:1

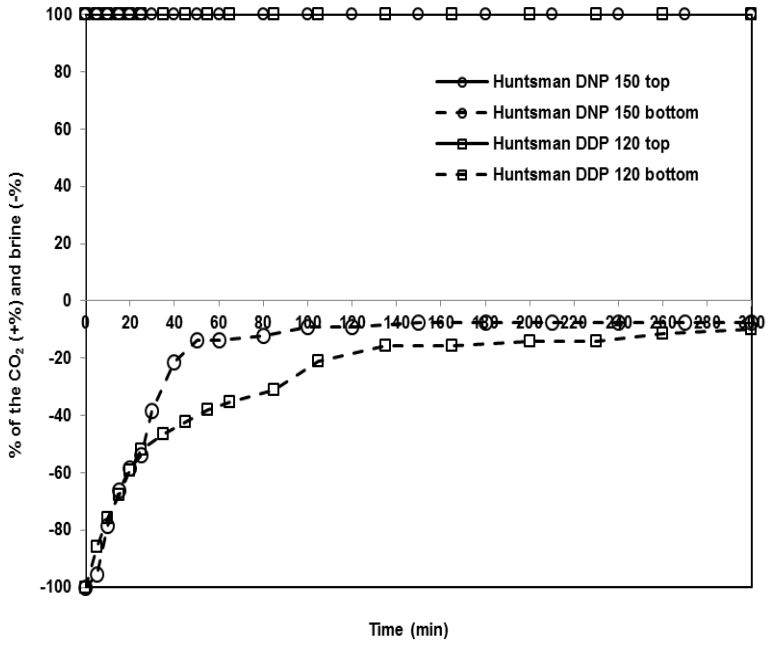

Figure 40. 0.03wt% Huntsman DDP 120 and DNP 150 in CO_2 at 1300psi and 25ºC, with brine (5wt%NaCl)/CO_2 volume ratio 1:1

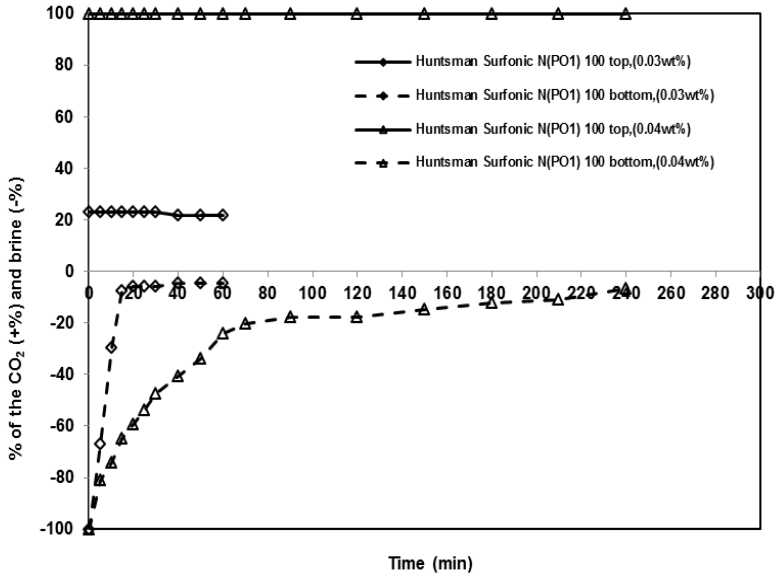

Figure 41. The foam stability of 0.03wt%, 0.04wt% Huntsman Surfonic N(PO1) 100 in CO_2 at 1300psi and 25°C, with a brine (5wt%NaCI)/CO_2 volume ratio 1:1

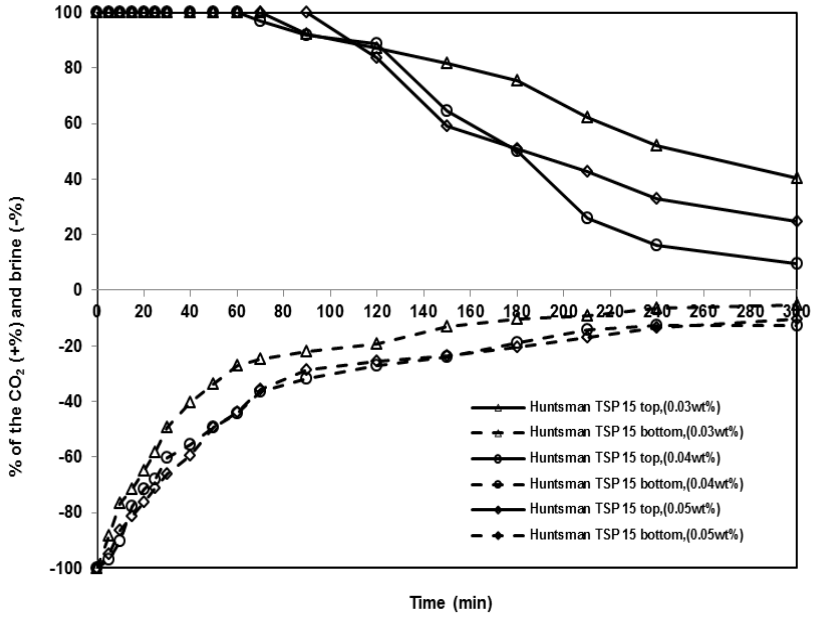

Figure 42. The foam stability of 0.03wt%, 0.04wt% and 0.05wt% Huntsman TSP 15, tristyrylphenol ethoxylates in CO_2 at 1300psi and 25°C, with a brine (5wt%NaCI)/CO_2 volume ratio 1:1

The Stepan CO710 has higher foam stability in CO_2-brine system than that of Stepan CO630, Figure 39, mainly because under the same pressure, less CO630 actually dissolved in CO_2. For Stepan CO710, after 280 minutes, approximately 10vol% of brine and all the liquid CO_2 still remains in the emulsion, meaning that it is an excellent foaming agent. Huntsman DDP 100 at a concentration of 0.03wt% was not capable of stabilizing foam. Both Huntsman DDP 120, branched dodecylphenol ethoxylate, and Huntsman DNP 150, a twin-tailed, branched, nonylphenol ethoxylate, were capable of stabilizing CO_2-in-brine foam at a concentration of 0.03wt%, as shown in Figure 40. After 300 minutes, the foam retained all of the CO_2 in the discontinuous phase and ~10% of the brine in the continuous films.

In summary, each of the water-soluble branched alkylphenol ethoxylates was capable of stabilizing CO_2-in-brine foams under the conditions of these tests. Nearly all of the foams were stable for 300 minutes, retaining all of the CO_2 and ~5 - 20% of the brine (~95–83% quality) at the end of the five hour test.

4.2 BRANCHED ALKYL ETHOXYLATES

4.2.1 Structures of branched alkyl ethoxylatyes

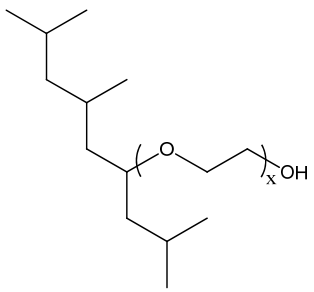

Figure 43. Structure of Dow trimethylnonyl Tergitol TMN 6 (x = ~8)

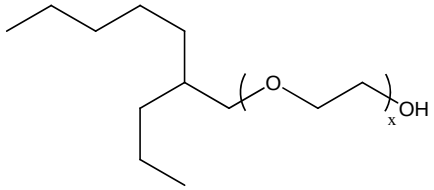

Figure 44. Structures of BASF Lutensol XP 70 (x = 7) and 80 (x = 8) (Guerbet alcohol-based C10 alkyl chain structure is proprietary, the structure above is our qualitative representation)

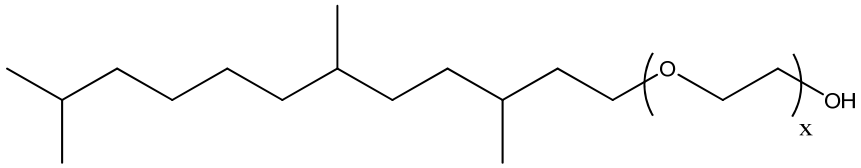

Figure 45. Structures of BASF Lutensol TO 8 and 10 iso C13 oxoalcohol ethoxylates and 8 or 10 EO groups (the structure above is our qualitative representation)

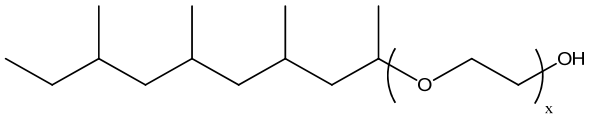

Figure 46. Structures of Huntsman isotridecyl ethoxylate TDA 8, TDA 9, TDA 11, x=8, 9 ,11 respectively, branched tridecyl alcohol ethoxylates with multiple methyl and/or ethyl branches on alcohol alkyl groups

4.2.2 Solubility results of branched alkyl ethoxylatyes

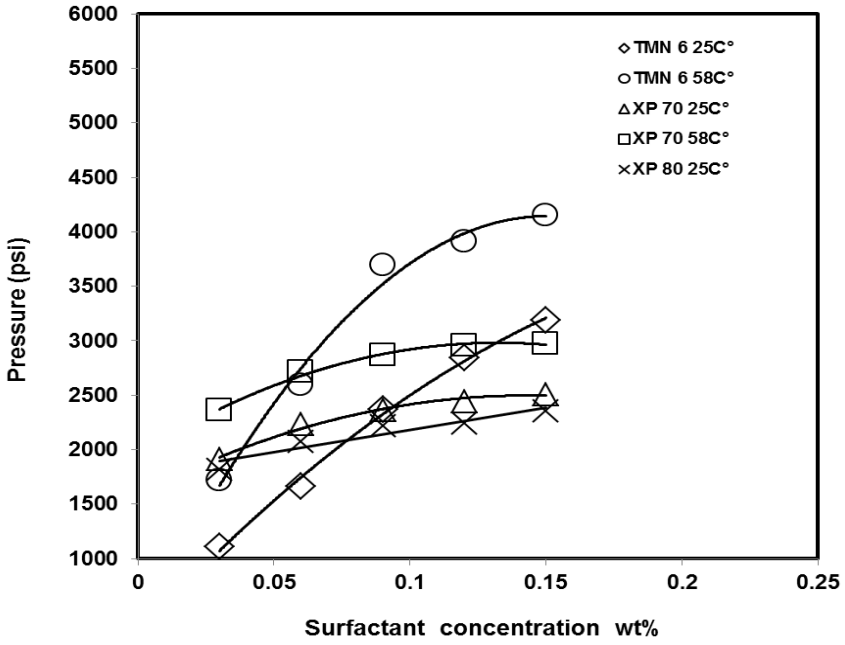

Figure 47. The solubility of TMN 6 and BASF XP 70 in CO_2 at 25ºC and 58ºC, XP 80 in CO_2 at 25ºC

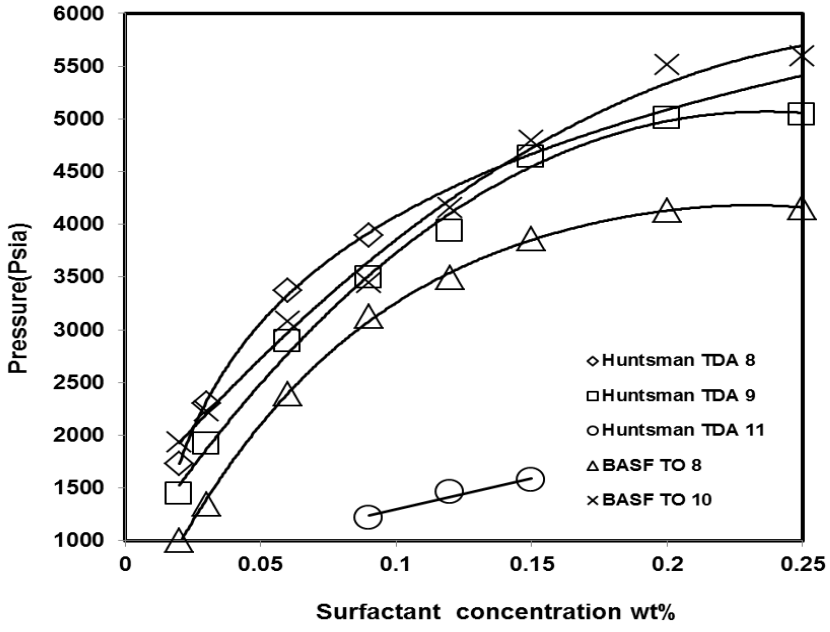

Figure 48. The solubility of BASF Lutensol TO 8, 10 and Huntsman TDA 8, 9 and 11 in CO_2 at 25 ºC

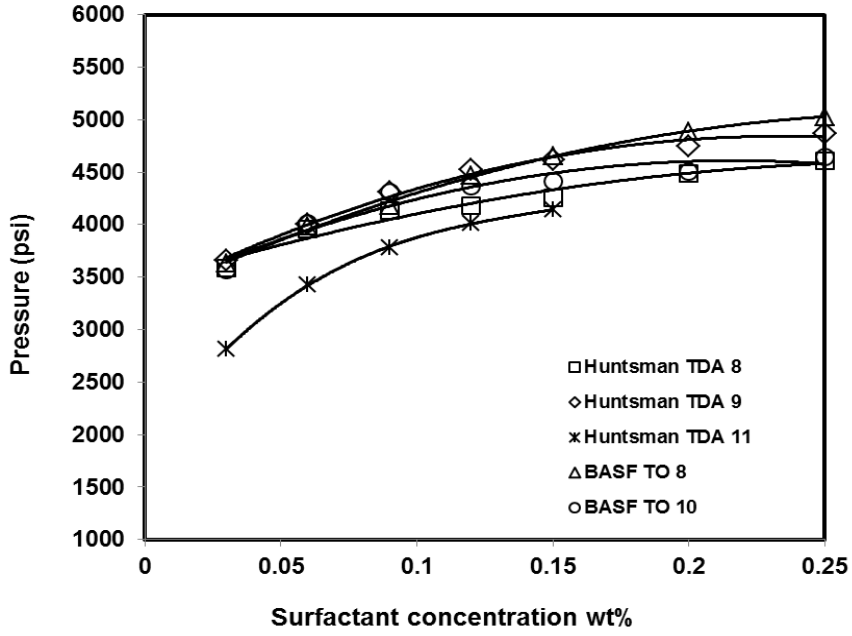

Figure 49. The solubility of BASF Lutensol TO 8, 10 and Huntsman TDA 8, 9 and 11 in CO_2 at 58°C

The solubility of the Dow's branched C_{12} TMN 6 alkyl ethoxylate is provided in Figure 47. This surfactant product (10% water) was not dehydrated prior to use. The cloud point curve occurs at lower pressures than the branched alkylphenol ethoxylates, apparently due to the lower molecular weight and the absence of the somewhat CO_2-phobic aromatic ring. The solubility reported in Figure 47 is also lower than that reported by Johnston and co-workers (Ryoo 2003) [11], who measured the cloud point pressure of a dehydrated 0.5wt% solution of TMN 6 in CO_2 to be about 1200psi (~8.3MPa) at 25°C and about 3000psi (~20.7MPa) at 65°C. Although this difference may be due in part to the absence of water in the sample of TMN 6 used by Johnston's group, it is also likely due to the difference in techniques used to determine the cloud point pressure.

The solubility of BASF's branched C_{10} Lutensol XP 70 and 80 alkyl ethoxylates at 25°C and 58°C is illustrated in Figure 47. The solubility of Lutensol XP 70 and XP 80 in CO_2 is

comparable to that exhibited by Tergitol TMN 6. Figure 48 illustrates the cloud point loci at 25°C of BASF branched C_{13} oxoalcohol Lutensol TO 8 and 10, and the Huntsman isotridecyl C_{13} ethoxylates TDA 8, 9, and 11.

In summary, the CO_2-solubility of the water-soluble, branched, alkyl (8–12 carbons) ethoxylates selected for this study are comparable in magnitude. Further, these surfactants are slightly more soluble in CO_2 than the branched alkylphenol ethoxylates when compared on an equal weight percentage basis. The surfactants are roughly 0.03–0.10wt% soluble in CO_2 in the 1300– 2000psi (9.0–13.8MPa) range at 25°C.

4.2.3 Foam stability results of branched alkyl ethoxylatyes

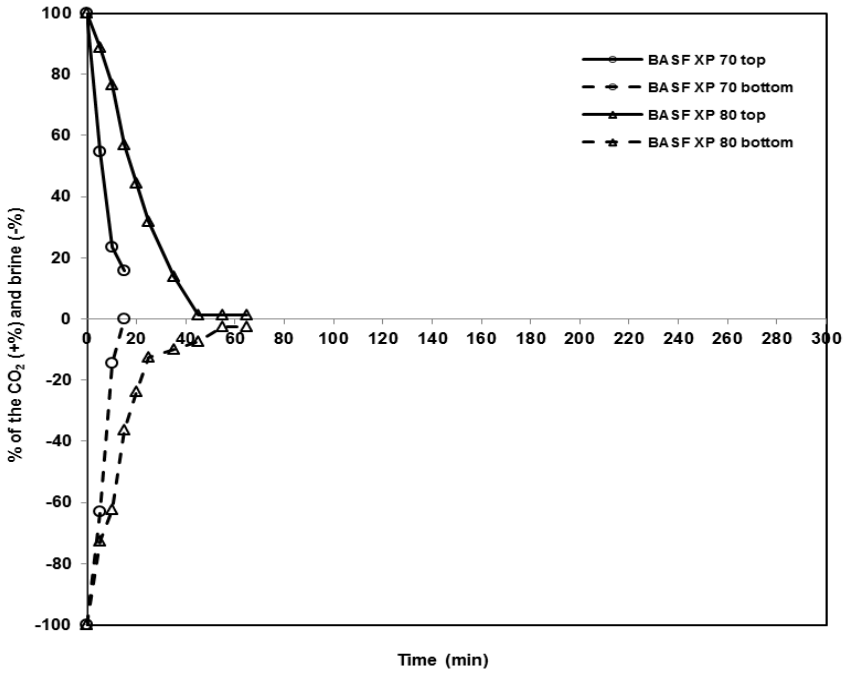

Figure 50. The foam stability of 0.04wt% BASF Lutensol XP 70 and BASF Lutensol XP 80 in CO_2 at 1300psi and 25 ºC, with a brine (5wt%NaCI)/CO_2 volume ratio 1:1

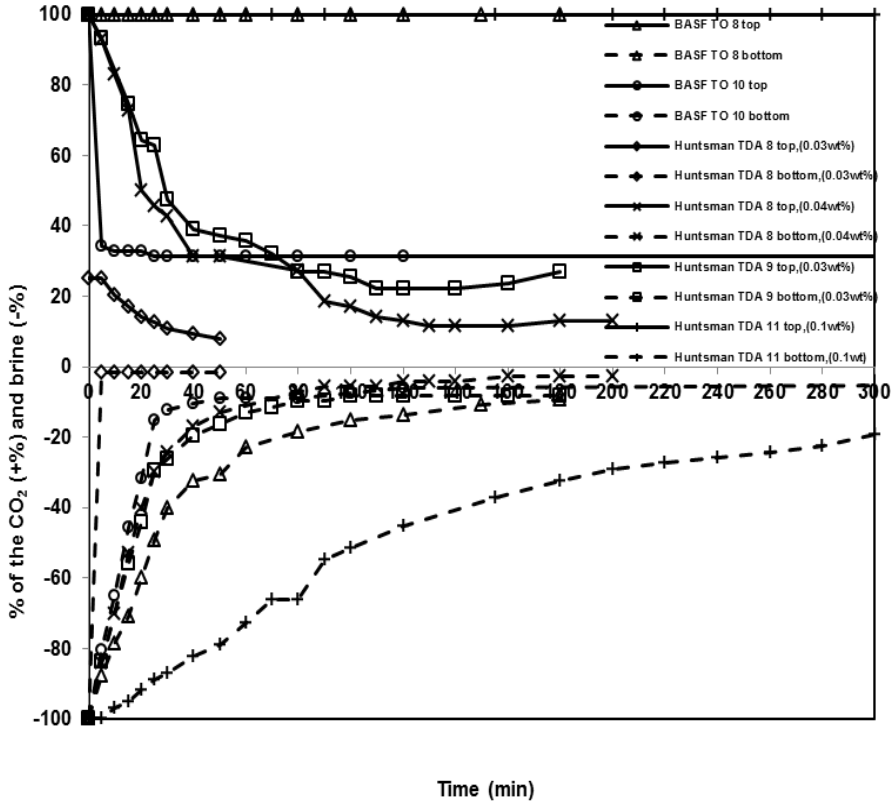

Figure 51. The foam stability of 0.03wt% BASF TO 8, 10, 0.03wt% and 0.04wt% Huntsman TDA 8, 0.03wt% Huntsman TDA 9, and 0.1wt% Huntsman TDA 11 in CO_2 at 1300psi and 25°C, with a brine(5wt%NaCI)/CO_2 volume ratio 1:1

The foam formed with the TMN 6 surfactant at a concentration of 0.04wt% collapsed within a minute. One experiment conducted with 0.04wt% BASF Lutensol XP 70 yielded foam that collapsed within a minute, and a second test of the same system yielded foam that collapsed within 15 minutes, Figure 50. Foam formed using 0.04wt% XP 80, which collapsed within about 45 minutes as shown in. The foam results for BASF TO 8 and 10 and Huntsman TDA 8 are shown in Figure 51. The BASF TO surfactants were capable of generating foams that were stable for several hours, although, for the case of BASF TO 10, a clear zone containing about 70% of the CO_2 appeared quickly. The Huntsman TDA 8, at a concentration of 0.3wt% of the

CO_2 mass, formed small foam that collapsed within an hour. Huntsman TDA 9 generated stable foam for 3 hours when present at a concentration of 0.03wt%. TDA 11 provided the most stable foam in Figure 29 when its concentration was raised to 0.1wt%. The Huntsman KR 8 surfactant was not capable of generating foam at 0.02wt%.

In summary, the branched ethoxylated alcohols were, as a whole, not as effective as the branched alkylphenol ethoxylates in stabilizing CO_2-in-brine foams under the test conditions associated with this study. Several surfactants, such as the BASF TO surfactants, did yield promising results, however. Therefore, branched alkyl ethoxylates (i.e. ethoxylated alcohols) may also be viable CO_2-soluble surfactants for generating CO_2-in-brine foams.

4.3 FATTY ACID-BASED SUFACTANTS AND LINEAR ALYKYL ETHOXYLATES

4.3.1 Structures of fatty acid-based surfactants and linear alkyl ethoxylatyes

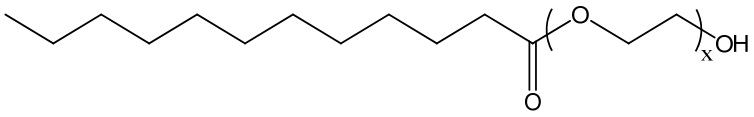

Figure 52. Structure of Monolaurate polyethyleneglycol, Sigma Aldrich PEG monolaurate 600 (x = 9)

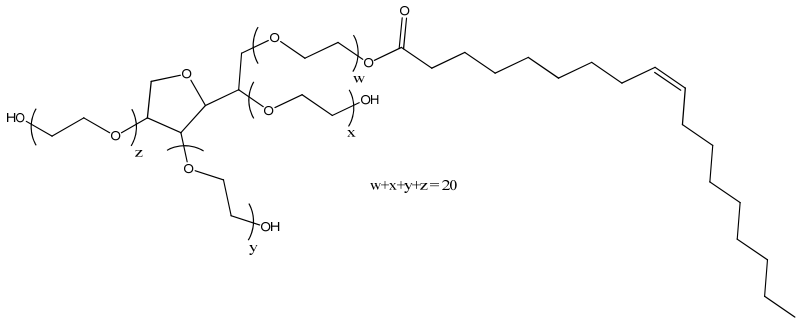

Figure 53. Structure of Sigma Aldrich Polyoxyethylene (20) sorbitan monooleate, Tween 80

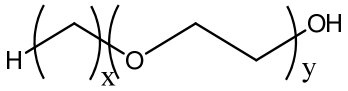

Figure 54. Structures of Huntsman L 12-8, the eight-mole ethoxylates of linear, primary C10-12 alcohol, (x ~ 12, y = 8), BASF Lutensol AO 8, AO 11, (x ~ 13.7, y = 8, 11), saturated, predominantly unbranched C_{13-15} oxo alcohol that consists of 67% C_{13} and 33% C_{15}

4.3.2 Solubility results of fatty acid-based surfactants and linear alkyl ethoxylatyes

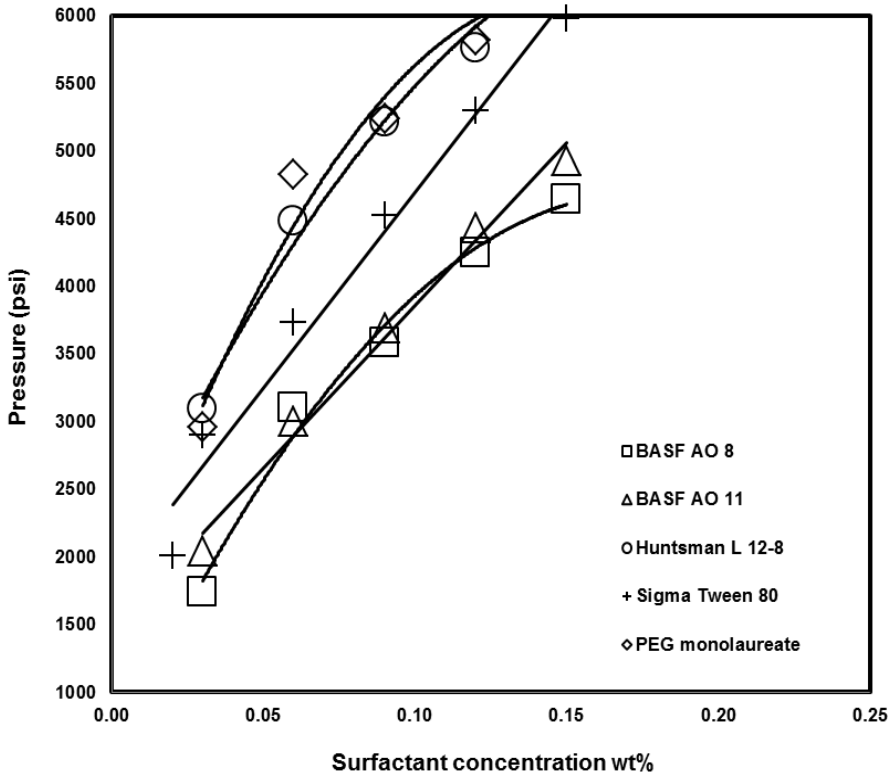

Figure 55. The solubility of Huntsman L 12-8, BASF AO 8, 11, Sigma Tween 80 and PEG monolaureate in CO_2 at 25 ºC

The cloud point curves for polyethene glycol monolaurate and Tween 80 in CO_2 at 25^{o}C are provided in Figure 55. Due to the significantly larger hydrophile and hydrophobe, the Tween 80

exhibits a markedly higher cloud point pressure over most of the composition range, although the difference becomes less significant at the most dilute concentrations. The solubility values for Tween 80 at 25°C are lower than those reported by Johnston and co-workers, who reported that 1.0 and 0.5wt% Tween 80 could be dissolved in CO_2 at 25°C and 3500 or 2300psi, respectively. When we replicated these temperature, pressure and composition conditions, however, a very small liquid phase was observed at the bottom of the sample volume (i.e. two-phase liquid-fluid equilibrium). When the pressure was elevated to 10,000psi and the mixtures were stirred for 15 minutes, a very cloudy translucent mixture resulted. Transparent, clear, homogeneous solutions could only be realized at the more dilute concentrations defined by the cloud point curve shown in Figure 55.

4.3.3 Foam stability results of fatty acid-based surfactants and linear alkyl ethoxylatyes

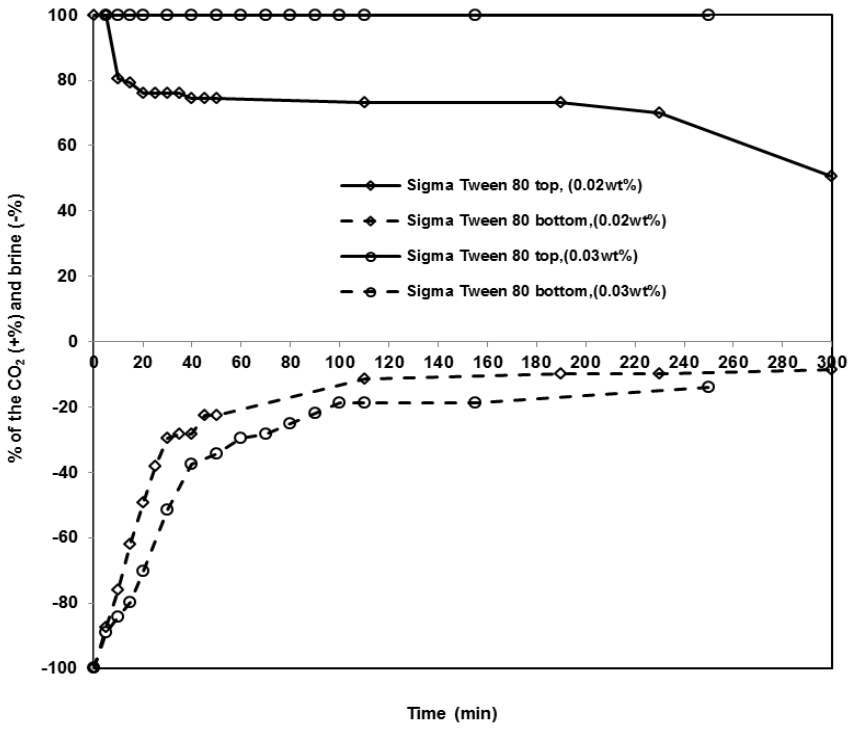

Figure 56. The foam stability of Sigma Tween 80 in CO_2 at 1300psi and 25°C, with a brine (5wt%NaCI)/CO_2 volume ratio 1:1

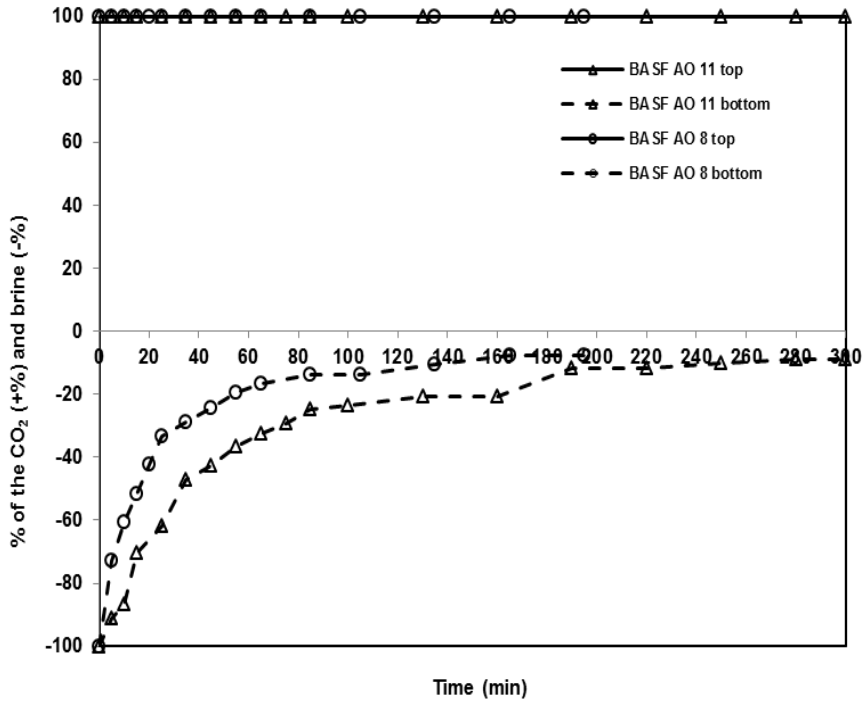

Figure 57. The foam stability of 0.03wt% BASF AO 8 and AO 11 in CO_2 at 1300psi and 25 ºC, with a brine (5wt%NaCI)/CO_2 volume ratio 1:1

A CO_2-in-brine foam could not be stabilized by poly(ethylene glycol) monolaurate at 0.03wt%. Despite its relatively high cloud point pressure curve, the Tween 80 surfactant was capable of stabilizing foam at a concentration of only 0.02wt%, the saturation concentration at 25^{o}C and 1300psi, as shown in Figure 56. In this case, a clear zone of CO_2 and a clear zone of brine grew after mixing stopped, and after 300 minutes about 50% of the CO_2 and 10% of the brine were retained in the emulsion. When the amount of Tween 80 charged to the vessel was 0.03wt% of the CO_2 (a concentration greater than the saturation concentration at these conditions) the foam stability was enhanced to a level similar to that exhibited by the branched alkylphenol ethoxylates, but Tween 80 is less CO_2-soluble than the branched alkyl phenol ethoxylates at

concentrations of 0.03wt% and higher. Therefore, fatty acid-based surfactants may also serve as viable CO_2-soluble candidates for stabilizing CO_2-in-brine foams.

Huntsman L12-8 does not stabilize foam when present at a concentration of 0.03wt%. BASF AO 8 was not capable of stabilizing foam at 0.02wt%. BASF AO 11 at a concentration of 0.03wt% was capable of generating stable foam that retained all of the CO_2 and about 10% of the brine after 300 minutes, Figure 57.

4.4 EFFECT OF CO_2: BRINE VOLUMETRIC RATIO ON THE FOAM STABILITY

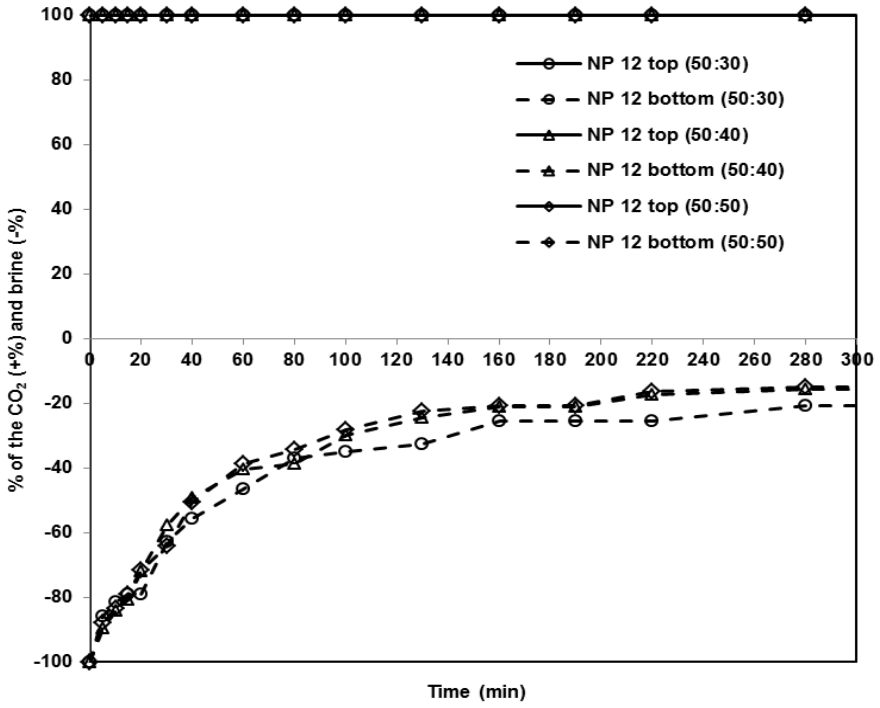

Figure 58. Effect of CO_2: brine volumetric ratio on the foam stability test, the volumetric ratio is provided in the parentheses of the legend. The solid lines represent the top of the emulsion phase, while the dashed curves represent the bottom of the emulsion phase.

The best surfactants had the most stable foam and slowly growing clear zones of brine and then CO_2, while the surfactants with poorer stabilizing abilities had an emulsion that collapsed within seconds or minutes. It is possible to conduct this screening test with other ratios of brine and CO_2, however. Tests with Dow Tergitol NP 12, a highly branched nonylphenol ethoxylate with 12 EO groups, were conducted using liquid CO_2: brine volumetric ratios of 50:50, 50:40, 50:30, 50:20 and 50:10. There was not enough brine present in the 50:10 and 50:20 experiments to form foam using this technique, however. The results for the other ratios of 50:50, 50:40 and 50:30, provided in Figure 58, are in good qualitative agreement when compared on a basis that compares the percentage of the total brine that is present in the clear zone. Further, these results indicate that Dow Tergitol NP 12 generates very stable foam; after 5 hours all of the CO_2 and ~20% of the brine are retained in the CO_2-in-brine emulsion.

4.5 FOAM STABILITY RESULTS WITH SACROC BRINE

In the previous section, the ability of different types of foaming agents to form stable foam in CO_2/5wt% brine solution was demonstrated. Several excellent candidates were chosen for the same experiments but in the real reservoir solution, SACROC brine, which is from one of Kindermorgan's (oil company in Texas) pilot oil reservoir. They are Huntsman Surfonic N series, BASF Lutensol TO 10, and Huntsman TDA 11.

A produced SACROC brine sample (specific gravity 1.059, pH 6.84) from this field containing 83078ppm TDS (major constituents 48762ppm Cl^-, 25850ppm Na^+, 916ppm Mg^{+2}, 4345ppm Ca^{+2}, 274ppm Sr^{+2}, 2133ppm HCO_3^-, 798ppm SO_4^{-2}) was filtered with 0.22 micron

cellulose acetate paper prior to use. Based on the solubility results for these surfactants at 58°C and 3200psi, 0.02–0.03wt% of the surfactant relative to the mass of CO_2 was used. And the results are shown below:

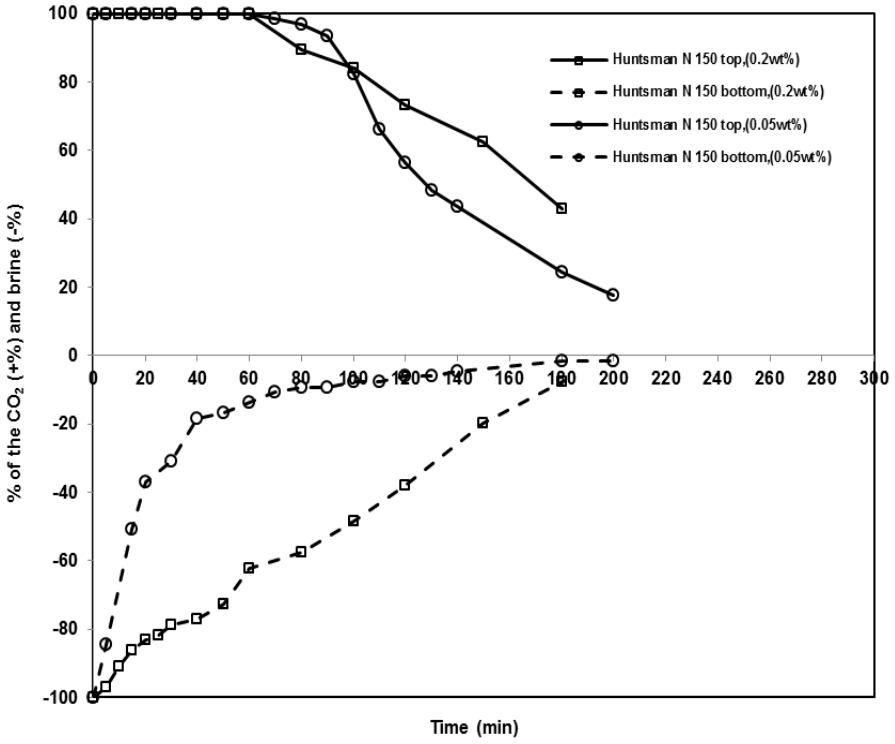

Figure 59. The foam stability of 0.05% and 0.2wt% Huntsman N 150 in CO_2 at 3200psi and 58°C, with SACROC/CO_2 brine volume ratio 1:1

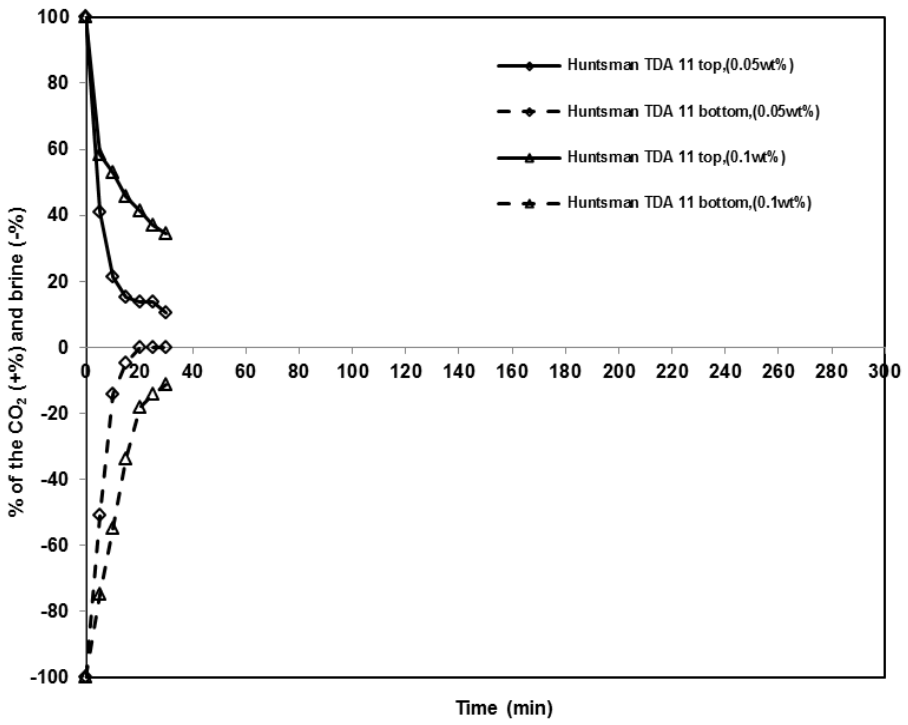

Figure 60. The foam stability of 0.05% and 0.1wt% Huntsman TDA 11 in CO_2 at 3200psi and 58°C, with SACROC brine/CO_2 volume ratio 1:1

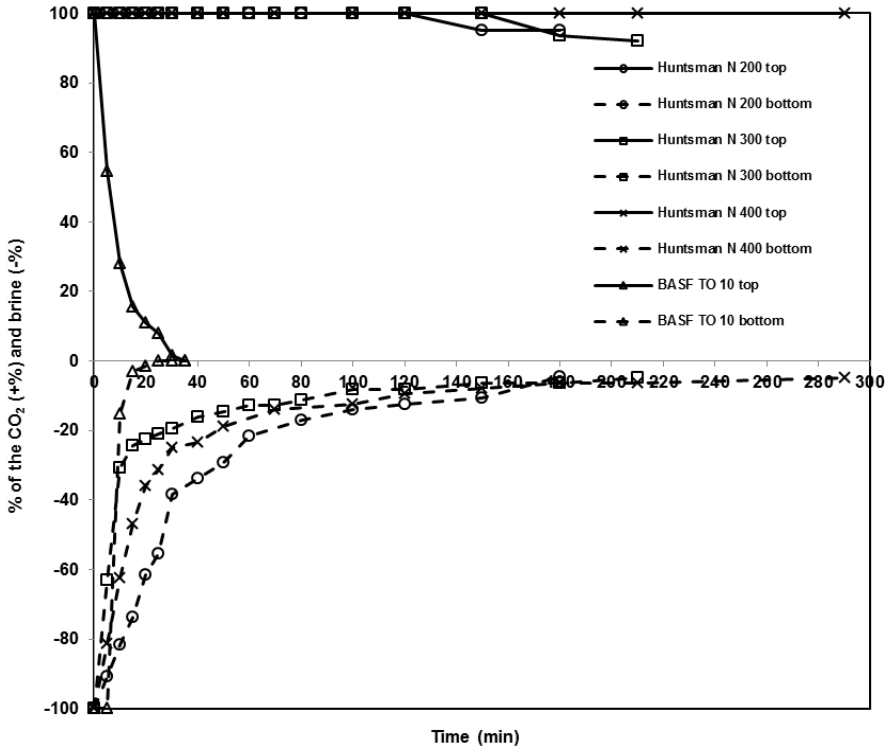

Figure 61. The foam stability of 0.03wt% Huntsman N 200, Huntsman N 300, Huntsman N 400, and BASF TO 10 in CO_2 at 3200psi and 58ºC, with SACROC brine/CO_2 volume ratio 1:1

The foam stability results for the SACROC brines obtained with the Huntsman Surfonic surfactants, TDA 11, and BASF TO 10 are provided in Figure 59-61. The Huntsman Surfonic N surfactants generated foams that were more stable than those formed with BASF TO 10. As the length of the ethoxylated hydrophile increased from 12 to 20 EO groups in the Huntsman series, the foams became more stable. The foams were less stable than those obtained using the same surfactants in the screening tests due to the increased temperature (58ºC vs 25ºC), the increase in the TDS of the brine (83078 ppm vs 50000 ppm), and the mixed ions present in the SACROC brine (Cl^-, Na^+, Mg^{+2}, Ca^{+2}, Sr^{+2}, HCO^{3-} , $SO4^{-2}$ vs Na^+, Cl^-). Nonetheless the foam stability results indicate that these surfactants, especially branched alkylphenol ethoxylates, do have the potential to form foams at reservoir conditions.

5.0 CO_2 MOBILITY CONTROL RESULTS OF CO_2-FLOODING THROUGH POROUS MEDIA EXPERIMENTS

An NETL-built flow-through-porous medium apparatus, rated to 4000 psi (27.7MPa) and shown in Figures 8 and 62, was used to collect the pressure drop data for CO_2 flowing through a dry core, and for neat CO_2 or CO_2/surfactant solution flowing into an initially brine-saturated or surfactant solution-saturated core at room temperature (~23^oC). The Berea sandstone core was wrapped in aluminum foil and then placed within a Buna-N sleeve. The core and sleeve were then placed inside the Temco (Model DCHR-1.0) core holder. Water was used as the overburden fluid to prevent annular flow of the fluids between the core and the inner surface of the sleeve. The overburden water pressure was maintained at ~500 psi (~3.5MPa) above the CO_2 pressure by using the High Pressure Equipment Company manual water pump (Model 62-6-10). CO_2 was initially pressurized to the desired pressure of ~2700psi with the Haskel gas booster pump (Model AGD-75-C8), filling the windowed Thar Technologies stirred cell (104cm^3, Model R100), the core holder, the separator used to collect water that is displaced from the core, and the two coupled Quizix positive displacement pumps (270 cm^3 per cylinder, Model C-6000-10K). If surfactants were to be dissolved in the CO_2, the surfactants would be loaded into the stirred cell prior to pressurization and mixed with CO_2 with the magnetically coupled stirrer until the solution was transparent.

During a mobility test, the first positive displacement pump was then engaged at a constant discharge volumetric flow rate, which resulted in the displacement of neat CO_2 from the pump into the continuously stirred cell. For tests conducted with surfactant initially dissolved in the CO_2 retained within the stirred cell, this resulted in a small amount of dilution of the surfactant solution. For example, the pore volume of the core was only ~13 cm^3 and the stirred cell volume was 104 cm^3, therefore the injection of a pore volume of CO_2 into the stirred cell during the mobility test would reduce the surfactant concentration from 0.060wt% to 0.053wt%. The CO_2 or CO_2/surfactant solution leaving the stirred cell flowed into the core. The core effluent was directed into the Swagelok separator (300cm^3, Model 316L-50DF4-500) in which brine displaced from the core would accumulate. The CO_2 leaving the top of the separator was then received by the second positive displacement pump, which was engaged at the same flow rate as the first pump but in the receiving mode. The CO_2 pressure was measured using the recycle pump analog transducers (from Sensata Technologies) and the Swagelok pressure transducers (Model PTI-S-AG400-12AV) and the pressure drop along the core sample was measured by aValidyne differential pressure transducer (Model DP303-26). The data acquisition was achieved using the Quizix and Validyne controllers and the National Instruments LabVIEW software.

Figure 62. Photograph of the NETL mobility apparatus

Pneumatic compressor (on floor, left), horizontal dual PD pumps and PC for process control and data collection (left), Thar windowed vessel for mixing CO_2 and surfactant (in plexiglas hood, left side) and knockout trap (in Plexiglas hood, right side), differential pressure transducers and Temco core holder (right).

All mobility tests were conducted at ~ 23^{o}C and 2700psi using a Berea sandstone core with a porosity of 17%. The injection and withdrawal rates of the coupled positive displacement pumps were maintained at 1 cm^3/min. The results for pressure drop across the entire 6" length of the core as a function of pore volumes (PV) of CO_2 injected are presented in Figure 63.

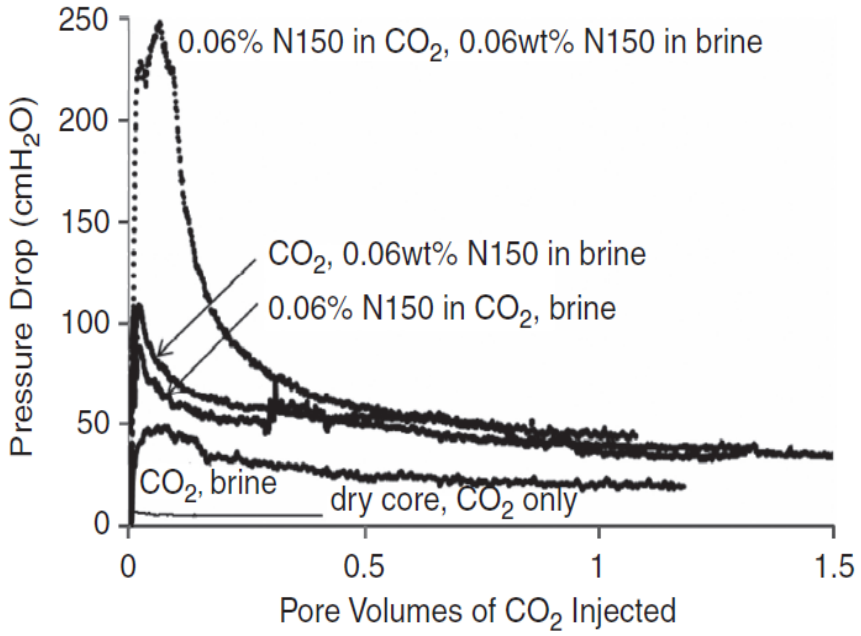

Figure 63. Pressure drop across a 6" long, 1"diameter, 104 md Berea sandstone core, 25°C, ~2700 psi, 1 cm^3/min volumetric flow rate (superficial velocity of 10ft/day)

The initial test was conducted using only CO_2 in order to obtain the permeability of the core, which was determined to be 104md. Because of the presence of a second phase in this experiment, the pressure drop was essentially constant through the duration of this test.

The core was then evacuated and then saturated with 5wt% NaCl brine prior to being flooded with CO_2. The pressure drop results for this "no surfactant" test indicate an initial rise in pressure followed by a decline in pressure and an approach to a limiting value. This is a typical transient response for a brine-saturated core being flooded with CO_2.

The core was then re-saturated with 5wt% NaCl brine and then flooded with CO_2 that was saturated with Huntsman Surfonic N 150 (~0.06wt% or 600 ppm). The pressure drop for this displacement is roughly twice that of the "no surfactant" experiment throughout the duration of the test. This is indicative of in-situ generation of foam that is less mobile than CO_2. Nearly identical results were obtained when neat CO_2 was injected into the core saturated with brine that

contained 0.06wt% of the Huntsman Surfonic N 150 surfactant, indicating that comparable mobility control foams can be generated with the surfactant being introduced to either the CO_2 or the brine.

The core was then saturated with brine containing surfactant, and flooded with a CO_2-surfactant solution. The concentration of the Huntsman Surfonic N 150 was ~0.06wt% in both phases. The corresponding pressure drop provided the strongest indication that foam had been generated within the core.

The pressure drops associated with the experiments conducted with surfactant were 2-5 times greater than the pressure drop observed when no surfactant was used. Therefore the use of this particular non-ionic surfactant in the CO_2 and/or brine phases at a concentration of ~6000 ppm would be expected to yield relatively weak foams that would probably be most appropriate for mobility control while providing a modest degree of conformance control.

6.0 CT IMAGING RESULTS OF CO_2 INVADING BRINE-SATURATED POLYSTYRENE CORE

In order to prove whether the foaming candidates are able to control CO_2 mobility, the experiment of CT Imaging of CO_2 invading brine-saturated polystyrene core is performed at NETL (Morgan Town, U.S.). The experimental setup, including the CT scanner, core holder, and fluid pumps, is shown in Figure 64.

Figure 64. Medical CT scanner at NETL with core holder and flow pumps

A fourth-generation computed tomography (CT) scanner was used to image the CO_2-brine flow within initially brine-saturated polystyrene (PS) cores. PS cores were used within the CT scanner because of the lack of natural subcore variations that are typically exhibited by sandstone or carbonate cores; the synthetic formation of the polystyrene cores creates a homogeneous porous medium. The lack of channeling or preferential flow through bedding

planes enables dynamic scanning of the front to be performed with greater ease within the CT scanner. The potential disadvantage of such a polymeric core is its oil-wet nature; in-situ foam-forming mechanisms are more conducive to water-wet porous media. Nonetheless, foam generation has been reported previously using oil-wet models (Lescure and Claridge 1986; Romero-Zeron and Kantzas 2007) or dolomite cores (Kuehne et al. 1992).

The various polystyrene cores have a porosity of about 10 - 20% and high permeability (tens of millidarcies), no bedding planes or natural heterogeneities that would induce preferential flow paths, and an internal pore structure similar in appearance to sandstone. A 5wt% potassium-iodide (KI) brine solution was used to initially saturate the 1.5 inch diameter, 6 inch long cores (174 cm^3 total volume) prior to CO_2 injection. KI has a greater attenuation than many other brine constituents, such as NaCl, which created a greater contrast between brine and CO_2 in the scans. Further, the surfactant used in the CT imaging study was capable of stabilizing CO_2-in-5wt% TDS brine, whether the dissolved ion pair was NaCl or KI. The core was saturated with brine prior to being placed in the core holder. All liquid CO_2 flooding experiments were performed at room temperature with a constant CO_2 injection rate of Q = 0.2 ml/min (superficial velocity = Q/cross-sectional area = 10 in/day = 0.829ft/day) with pore pressures from 2050 to 2200psi (~14.1–15.2MPa), confining pressures 250 psi (~1.7MPa) greater than the pore pressure.

Three different tests were conducted at ~2700 psi and 23^oC. First, a control experiment was performed with CO_2 invading a 5wt% KI brine saturated core; no surfactant was used. Second, the core was saturated with 1wt% Huntsman Surfonic N 150 dissolved in the 5wt% KI brine that saturated the core, but no surfactant was added to the CO_2. In the third test, the CO_2 was saturated with the surfactant (0.06wt% Huntsman N 150) in a windowed mixing vessel and the CO_2-rich solution was injected into the 5wt% KI brine saturated core.

For these experiments, a voxel size of 0.25mm x 0.25mm x 5mm was used to capture the dynamically advancing CO_2 with the CT scanner. The relatively large slice depth (5mm) was used so that the approximately 30 slices required to capture the entire core would take less than four minutes, and multiple full core scans could be conducted during each experiment. Slices along the length of the core are shown in the following figure for all three experiments at the beginning, middle and end of each experiment, as shown in appendix A. In these images (where the CO_2 has been shown in darker shades of purple with a false coloring scheme) the inclusion of the surfactant (B) and (C) produced stable flow of CO_2 down the length of the core. Fingering of CO_2 occurred only in (A), the case in which no surfactant was used. Fingering was inhibited in the case of the surfactant dissolved in the CO_2 (B), or with 1.0wt% surfactant dissolved in the brine (C).

This difference in the ability of the injected CO_2 to displace brine with and without the addition of the surfactant is also shown in the appendix B for the experiment with no surfactant (A), surfactant in the brine (B), and surfactant added to the injected CO_2 (C). In case (A), the mean CT number (CTN), which is related to the average density in each CT slice, decreases gradually over time, with the largest decreases occurring at the injection side of the core as the fingers of CO_2 propagate through the PS core. This gradual change reflects the absence of a CO_2 front and the likely presence of CO_2 fingers. In contrast, the propagation of the CO_2/surfactant mixture is shown to stable and 'piston-like' for experiments (B) and (C), with the mean CTN per slice exhibiting low values in the CO_2-rich region behind the front, and high values in the brine ahead of the front, with a relatively short distance (i.e. sharp front) separating the two zones.

7.0 SUMMARY AND CONCLUSION

This work represents the first direct evidence of the formation of anisotropic microemulsion aggregation in liquid CO_2. High-pressure viscometry measurements show that this is also the case in liquid CO_2 with distinct increases in viscosity at ~6wt% Ni(di-HCF4)$_2$. Viscosity increases of 20–90% over shear rates 6000 – 11000 s^{-1} were attained using 6–10wt% of either the Co(di-HCF4)$_2$ and Ni(di-HCF4)$_2$ surfactants. In contrast, the spherical micelle-forming Na(di-HCF4) surfactant resulted in only minor viscosity increases of ~10%, even at concentrations up to 10wt%. It also demonstrates that knowledge gained from studies in hydrocarbon oils can be extended to more unusual solvents such as CO_2, provided surfactant solubility can be enhanced. The increase in viscosity is too small to be suitable for direct applications in enhanced oil recovery; however, the work does reveal an important principle: the viscosity of CO_2 can be controlled using surfactant self-assembly. As such this work provides a greater understanding of how the viscosity of this molecularly simple, but most uncooperative, solvent can be tuned with rod micelle-forming surfactants. Attention should now focus on design and synthesis of non-fluorous, commercially viable and more environmentally responsible, hydrocarbon surfactant alternatives which will lead to increased applications of CO_2-based technologies. There has been an exciting recent development in the field of CO_2-compatible hydrocarbon surfactants[31], anionic sodium amphiphiles bearing three t-butyl tipped chains aggregate to form spherical hydrated

reverse micelles. If tri-chain surfactants of this kind can be encouraged to grow anisotropically, these may serve as foundations for a new class of CO_2 fluid modifiers.

Several commercially available, hydrocarbon-based, nonionic, water-soluble surfactants exhibit sufficient solubility in CO_2 (0.02–0.10wt %) at typical MMP conditions to stabilize CO_2-in-brine emulsions formed in an agitated, windowed, high pressure cell. Examples of promising surfactants include branched alkylphenol ethoxylates (e.g.,Huntsman SURFONIC N-120, 150, and 200), branched alkyl ethoxylates (e.g.,Huntsman SURFONIC TDA-10 and 11 and BASF TO 10), a fatty- acid based surfactant, a predominantly linear ethoxylated alcohol, and experimental alkylphenol and styrylphenol surfactants. Transient mobility measurements indicated that weak foams were formed in brine-saturated Berea sandstone (approximately 100 md) when 0.06wt% SURFONICVR N 150 was dissolved in the CO_2. The pressure drop across the core (10ft/D superficial velocity) that occurred when the surfactant solution was introduced to a brine-saturated core was roughly twice the value measured when no surfactant was used. Similar results were observed when 0.06wt% of the surfactant was added only to the brine phase that initially saturated the core, and the greatest mobility reduction occurred when the surfactant was present in both the brine and the CO_2. This level of mobility reduction appears to be more commensurate with mobility control than conformance control. CT imaging using PS cores substantiated that despite the oil-wet nature of the porous medium, the injection of a CO_2/SURFONIC N-150 solution (0.06wt%) into a brine-saturated core resulted in the formation of foams in situ characterized by distinct foam front and the complete suppression of viscous fingers. Similar results were observed when the surfactant was introduced only to the brine initially saturating the core. The results of this work, along with the recent findings of Johnston and coworkers, indicate that there are many commercially available, water-soluble, nonionic

surfactants that not only can dissolve in CO_2 in appreciable amounts (approximately 0.02–0.10wt%), but also stabilize CO_2-in-brine foams in situ. The availability of such surfactants provides added flexibility for CO_2 mobility control using foams. In a conventional SAG process using a CO_2-insoluble, water-soluble surfactant, the surfactant is added to the brine slugs that are usually injected alternately with CO_2 slugs. The CO_2-soluble, water-soluble, nonionic surfactants identified in this work would provide the operator with the additional options of adding the surfactant solely to the injected CO_2 (whether or not alternating slugs of brine are used), or adding surfactant to CO_2 slugs and to brine slugs.

According to our work, the best foam candidates should be nonionic, both water and CO_2 soluble, non-fluorous, efficacious at MMP but dilute in concentration and preferred as a liquid. The best type is apparently the branched alkyl phenol ethoxylate, especially with a branched alkyl chain containing 9~13 carbons and 8~15 EO groups. And the second best surfactants should be branched alkyl ethoxylates, also with a branched alkyl chain containing 9~13 carbons and 8~15 EO groups.

8.0 FUTURE WORK

Firstly, attention should now focus on design and synthesis of non-fluorous, commercially viable and more environmentally responsible, hydrocarbon surfactant alternatives which will lead to increased applications of CO_2-based technologies. There has been an exciting recent development in the field of CO_2-compatible hydrocarbon surfactants [44], anionic sodium amphiphiles bearing three t-butyl tipped chains aggregate to form spherical hydrated reverse micelles. If tri-chain surfactants of this kind can be encouraged to grow anisotropically, these may serve as foundations for a new class of CO_2 fluid modifiers.

Secondly, the morphology of water-in-CO_2 reversed micelles formed by different group metal cations (M^+) should also be investigated, in order to reveal intrinsic principles and rules in CO_2 direct thickeners design. Recently, Dr. Eastoe and co-workers synthesized a new type of CO_2 viscosifier, with different alkali metal cations and F7H4 ion [45].

These M-F7H4 surfactants were then investigated in water in-CO_2 microemulsions, forming reverse micelles, in which a range of micelle morphologies were observed, with Li-F7H4, Na-F7H4 and K-F7H4 all forming one dimensional aggregates, prolate ellipsoids, rods and ellipsoids respectively, whereas Rb-F7H4 forming isotropic spherical aggregates. High pressure viscometry shows that surfactants forming more anisotropic micelles give rise to higher CO_2 viscosity. For the first time, a clear quantitative link is shown between the chemical nature

of a surfactant additive and the enhancement of CO_2 viscosity. Therefore, it is possible to design specific optimized architectures for the important function of viscosity enhancement of CO_2.

Thirdly, there is an increasing focus on CO_2 mobility control using nanoparticles, which hopefully will be a promising type of CO_2-brine foaming agents. The University of Texas (Austin) is evaluating inexpensive alternative nanoparticle sources to provide the large volumes needed for foam stabilization in field-scale CO_2 floods. The study entails using low cost, commercially available "bare" silica nanoparticles and applying a polyethylene glycol (PEG) coating in-house to produce low-cost alternatives as well as the use of natural nanoparticles (e.g., fly ash) to develop CO_2 foam. A New Mexico Institute of Mining and Technology research activity is conducting complementary research on the use of nanoparticles to increase CO_2 flood sweep efficiency. The effects of particle retention on core permeability and porosity will be investigated using long-term core flooding experiments and nanoparticle-stabilized CO_2 foams. Additionally, surfactant molecule effects on the stability and performance of nanoparticle-based CO_2 foams will be examined and evaluated for field application.

APPENDIX A

CT SLICES OF CO_2 WITHIN PS CORES; CO_2 INLET DISTRIBUTOR AT TOP LEFT CORNER, CORE OUTLET AT BOTTOM RIGHT CORNER

(A) no surfactant; (B) surfactant in brine; (C) surfactant with injected CO_2.

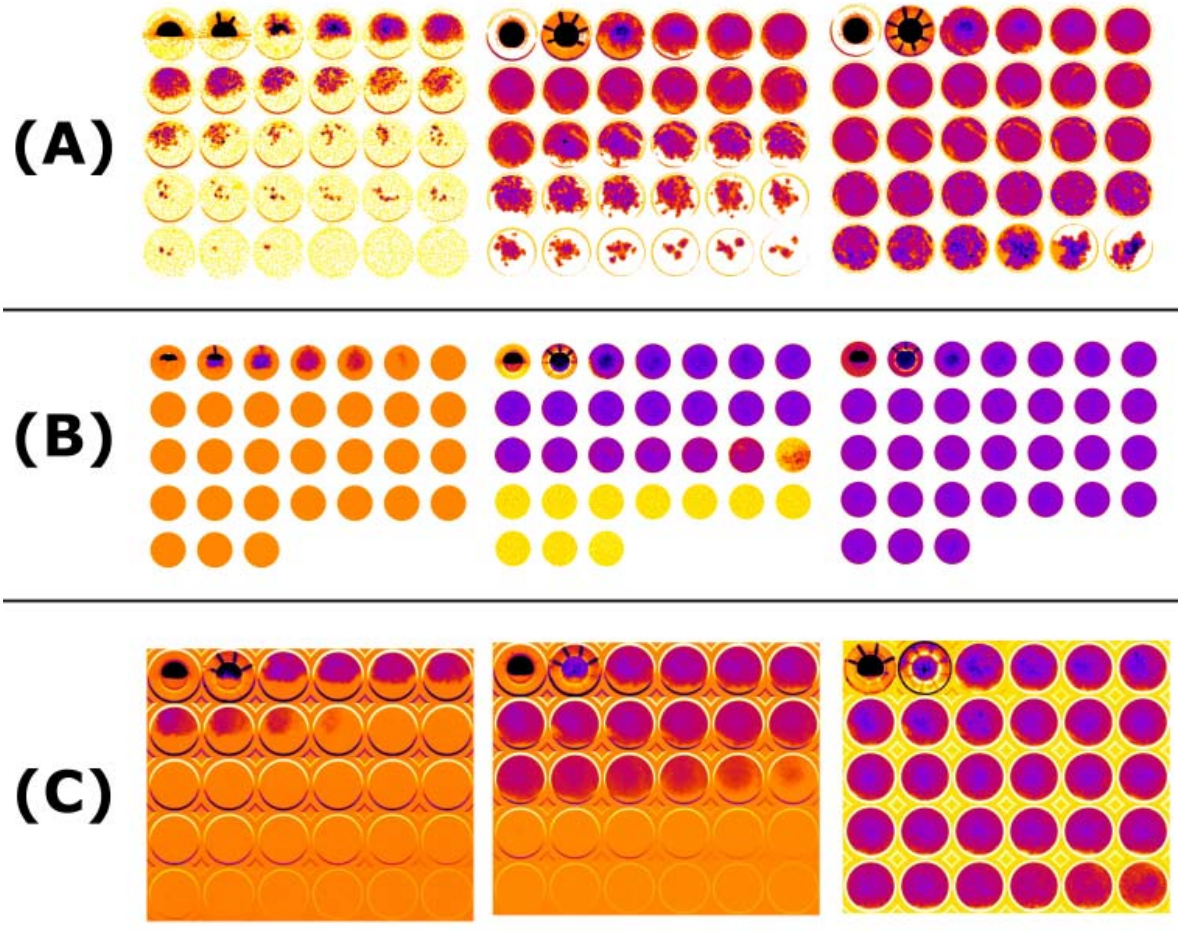

APPENDIX B

MEAN COMPUTED TOMOGRAPHY NUMBER (CTN) IMAGES

(A) No surfactant (B) Surfactant dissolved in the brine (C) Surfactant dissolved in the injected CO_2

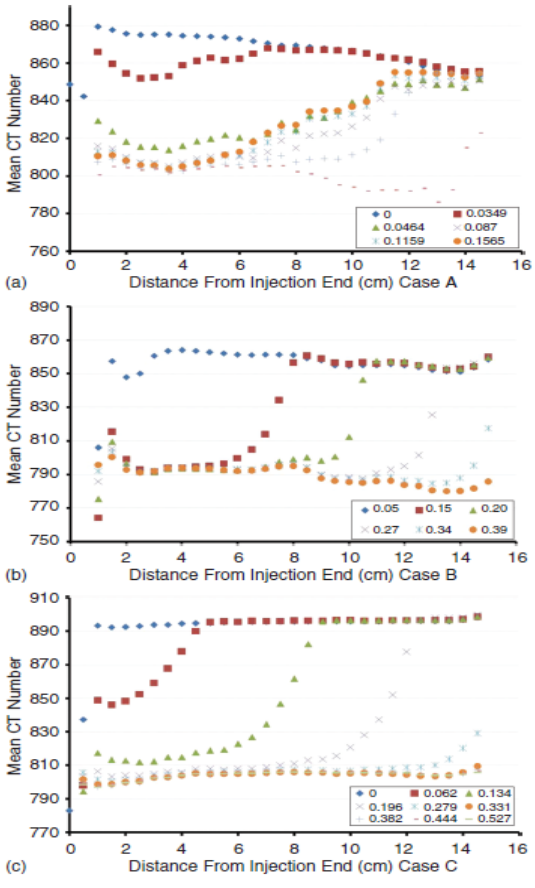

APPENDIX C

SANS PROFILES FOR EMULSIONS COLLECTED ON SANS2D AND LOQ ISIS

Data obtained at 1450psi and 77F in the HP-SANS pressure cell for Dow Tergitol NP-series surfactants and the Huntsman N 85 surfactant, also included is the profile for 1:1=CO_2: deuterated brine ratio

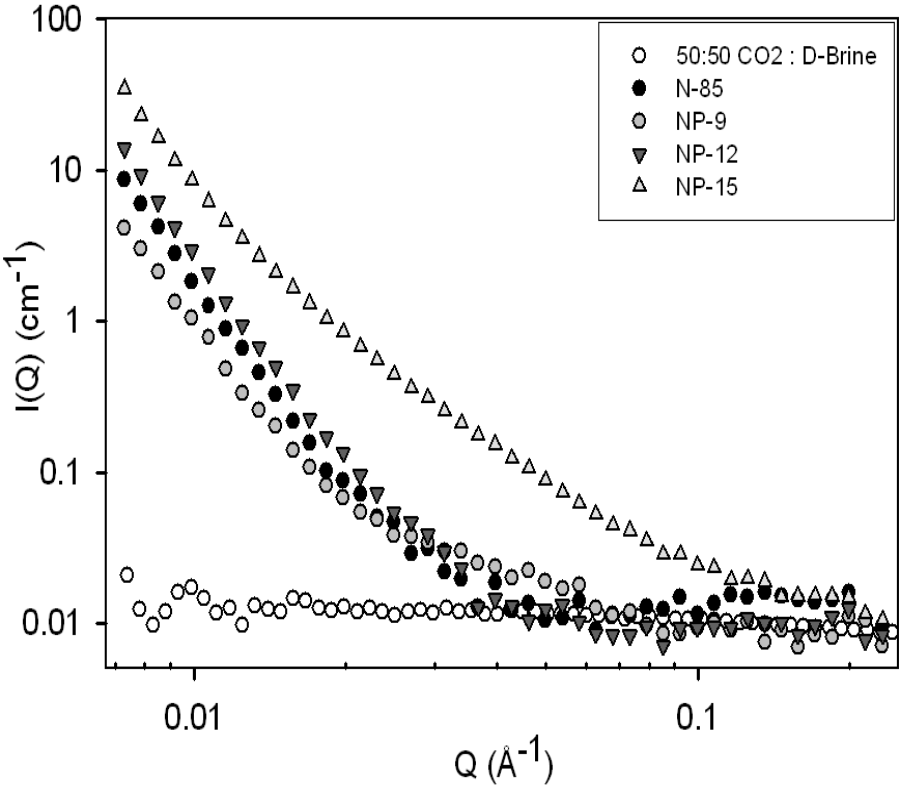

APPENDIX D

SANS PROFILES COLLECTED AT LOQ ISIS

Data obtained at 3200psi and 126F in the ISIS HP-SANS pressure cell, for Huntsman N150 with 1:1 CO_2:deuterated SACROC Brine (●), Hunstman N150 with 1:1 CO_2:D_2O (○), Hunstman N120 with 1:1 CO_2 : deuterated SACROC Brine (▼) and Huntsman N120 with 1:1 CO_2 : D_2O (▽). The inset shows the Porod curves and analysis for each of these profiles using the same symbols.

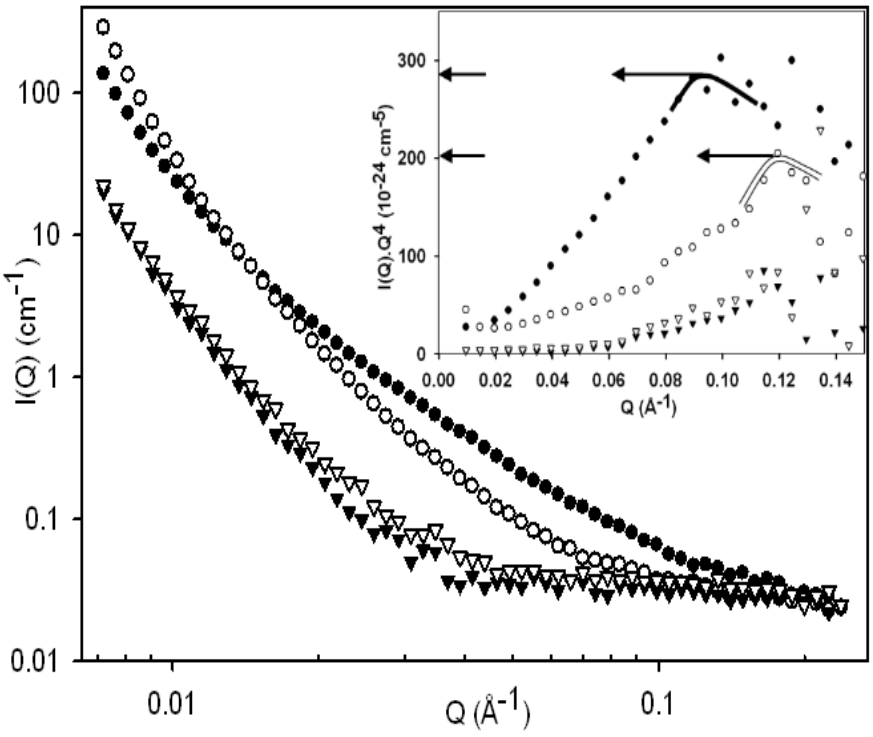

BIBLIOGRAPHY

1. Enick, R., A Literature Review of Attempts to Increase the Viscosity of Dense Carbon Dioxide, **1998**

2. The Foundation for Increased Oil Production and a Viable Domestic Oil Industry, U.S *Department of Energy*, **2006**

3. Holm, L. W.; Josendal, V. A., Mechanism of Oil Displacement by CO_2, *Journal of Petroleum Technology*, **1974**, 1427-36

4. Amarnath, A., Enhanced Oil Recovery Scoping Study, *Department of Energy*, **1999**

5. Xu, J., Jianhang Xu's Ph.D Dissertation, *University of Pittsburgh*, **2003**

6. Bernard, G.; Holm, L., Method for Recovering Oil from Subterranean Formations, *U.S. Patent 3342256*, **1967**

7. Irani, C., Solubilizing Surfactants in Miscible Drive Solvents, *U.S. Patent 4828029*, **1989**

8. Schievelbein, V., Method of Decreasing Mobility of Dense Carbon Dioxide in Subterranean Formations, *U.S. Patent 5033547*, **1991**

9. Bancroft, W.D., The Theory of Emulsification VI, *J. Phys. Chem.*, **1915**, 19, 275-309

10. Dhanuka, V.; Dickson, J.; Ryoo, W.; Johnston. K., High Internal Phase CO_2-in-Water Emulsions Stabilized with a Branched Nonionic Hydrocarbon Surfactant; *Journal of Colloid and Interface Science*, **2006**, 298, 406-418

11. Ryoo, W.; Webber, S.; Johnston, K., Water in Carbon Dioxide Microemulsions with Methylated Branched Hydrocarbon Surfactants, *Ind. Eng. Chem. Res.*, **2003**, 42, 6348-6358

12. Haruki, M.; Yawata, H.; Nishimoto, M.; Tanto, M.; Kihara, S.; Takishima, S., Study on Phase Behaviors of supercritical CO_2 including Surfactant and Water, *Fluid Phase Equilibria*, **2007**, 261, 92-98

13. Eastoe, J., Surfactant Chemistry, *Wuhan University Press*, **2003**

14. Eastoe, J.; Dupont, A.; Steytler, D.; Thorpe, M.; Gurgel, A.; Heenan, R., Micellization of Economically Viable Surfactants in CO_2, *Journal of Colloid and Interface Science*, **2003**, 258, 367-373

15. Eastoe, J.; Gold, S.; Rogers, S.; Wyatt, P.; Steytler, D.; Gurgel, A.; Heenan, R.; Fan, X.; Beckman, E.; Enick, R., Designed CO_2-Philes Stabilize Water-in-CO_2 Microemulsions, *Angewandte Chemie-International Edition*, **2006**, 22, 3675-3677

16. Eastoe, J.; Gold, S.; Steytler, D., Surfactants for CO_2, *Langmuir*, **2006**, 22, 9832-9842

17. Tabor, R.; Gold, S.; Eastoe, J., Electron Density Matching as a Guide to Surfactant Design, *Langmuir*, **2006**, 22, 963-968

18. Darocha, S.; Psathus, P.; Klein, E.; Johnston, K., Concentrated CO_2 in Water Emulsions with Nonionic Polymeric Surfactants, *Journal of Colloid and Interface Science*, **2001**, 239, 241-253

19. Le, V.; Nguyen, Q.; Sanders, A., A Novel Foam Concept with CO_2 Dissolved Surfactants, *SPE/DOE Improved Oil Recovery Symposium*, Tulsa, OK, April 19-23, **2008,** SPE-113370

20. Sanders, A.; Nguyen, Q.; Nguyen. N.; Adkins, S.; Johnston, K.P., Twin-tailed Surfactants for Creating CO_2-in-Water Macroemulsions for Sweep Enhancement in CO_2 EOR, *Abu Dhabi International Petroleum Exhibition and Conference*, Abu Dhabi, UAE, November 1-4, **2010**, SPE-137689-MS; doi: 10.2118/137689-MS

21. Adkins, S.S; Chen, X.; Chan, I.; Torino, E.; Nguyen, Q.; Sanders, A.; Johnston, K., Morphology and Stability of CO_2-in-Water Foams with Nonionic Hydrocarbon Surfactants, *Langmuir*, **2010**, 26(8), 5335–5348

22. Adkins, S.S.; Chen, X.; Nguyen, Q.P.; Sanders, A.W.; Johnston, K.P., Effect of Branching on the Interfacial Properties of Nonionic Hydrocarbon Surfactants at the Air-Water and Carbon Dioxide-Water Interfaces, *Journal of Colloid and Interface Science*, **2010**, 346, 455-463

23. Sanders, A., Successful Implementation of CO_2 Foam for Conformance Control, Dow Oil & Gas, *The 4th Annual Wyoming CO_2 Conference*, Casper, WY, June 29-30, **2010**; Sanders A.; Jones, R.; Mann, T.; Patton, L.; Linroth, M.; Nguyen, Q., Successful Implementation of CO_2-Foam for Conformance Control; *2010 CO_2 Conference*, Midland Texas, December 9-10, **2010**

24. Torino, E.; Reverchon, E.; Johnston, K.P., Carbon Dioxide/Water, Water/Carbon Dioxide Emulsions and Double Emulsions Stabilized With a Nonionic Biocompatible Surfactant, *Journal of Colloid Interface Science*, **2010**, 348, 469-478

25. Hollamby, M. J.; Trickett, K.; Mohamed, A.; Cummings, S.; Tabor, R. F.; Myakonkaya, O.; Gold, S.; Rogers, S.; Heenan, R. K.; Eastoe,J., Tri-Chain Hydrocarbon Surfactants as

Designed Micellar Modifiers for Supercritical CO_2, *J. Angew. Chem., Int. Ed*., **2009**, 48, 4993

26. Mohamed, A.; Trickett, K.; Chin, S.Y.; Cummings, S.; Sagisaka, M.; Hudson, L.; Nave, S.; Dyer, R.; Rogers, S.E.; Heenan, R.K.; Eastoe, J., Universal Surfactant for Water, Oils, and CO_2, *Langmuir Article; American Chemical Society*, **2010**, 26(17), 13861-13866

27. Terech, P.; Weiss, R. G., *Chem. Rev*., **1997**, 97, 3133

28. Nave, S.; Eastoe, J.; Heenan, R. K.; Steytler, D.; Grillo, I., *Langmuir*, **2000**, 16, 8741

29. Nave, S.; Paul, A.; Eastoe, J.; Pitt, A. R.; Heenan, R. K., *Langmuir*, **2005**, 21, 10021

30. Sagisaka, M.; Fujii, T.; Ozaki, Y.; Yoda, S.; Takebayashi, Y.; Kondo, Y.; Yoshino, N.; Sakai, H.; Abe, M.; Otake, K., *Langmuir*, **2004**, 20, 2560

31. Eastoe, J.; Gold, S.; Steytler, D. C., *Langmuir*, **2006**, 22, 9832

32. Steytler, D. C.; Thorpe, M.; Eastoe, J.; Dupont, A.; Heenan, R. K., *Langmuir*, **2003**, 19, 8715

33. Eastoe, J.; Fragneto, G.; Robinson, B. H.; Towey, T. F.; Heenan, R. K.; Leng, F. J., *J. Chem. Soc. Faraday Trans*., **1992**, 88, 461

34. Eastoe, J.; Towey, T. F.; Robinson, B. H.; Williams, J.; Heenan, R. K., *J. Phys. Chem*., **1993**, 97, 1459

35. Eastoe, J.; Steytler, D. C.; Robinson, B. H.; Heenan, R. K.; North, A. N.; Dore, J.C., *J. Chem. Soc. Faraday Trans*., **1994**, 90, 2497

36. Eastoe, J.; Paul, A.; Nave, S.; Steytler, D. C.; Robinson, B. H.; Rumsey, E.; Thorpe, M.; Heenan, R. K., *J. Am. Chem. Soc*., **2001**, 123, 988

37. Liu, Z. T.; Erkey, C., *Langmuir*, **2001**, 17, 274

38. Eastoe, J.; Paul, A.; Downer, A.; Steytler, D. C.; Rumsey, E., *Langmuir*, **2002**, 18, 3014

39. Eastoe, J.; Cazelles, B. M. H.; Steytler, D. C.; Holmes, J. D.; Pitt, A. R.; Wear, T. J.; Heenan, R. K., *Langmuir* , **1997**, 13, 6980

40. Shi, C. M.; Huang, Z. H.; Beckman, E. J.; Enick, R. M.; Kim, S. Y.; Curran D. P., *Ind. Eng. Chem. Res*., **2001**, 40, 908

41. Huang, Z.; Shi, C.; Xu, J.; Kilic, S.; Enick, R. M.; Beckman, E., *J. Macromolecules*, **2000**, 33, 5437

42. Xu, J.; Wlaschin, A.; Enick, R. M., *SPE Journal*, **2003**, 8, 85

43. Crossley,M. J.; Gorjian, S.; Sternhell, S.; Tansey, K. M., *Aust. J. Chem*., **1994**, 47, 723-738

44. Hollamby, M. J.; Tricket, K. J.; Mohamed, A.; Cummings, S.; Tabor, R.; Myakonkya, O.; Gold, S.; Rogers, S.; Heenan R. K.; Eastoe, Tri-chain Hydrocarbon Surfactants as Designed Micellar Modifiers for Supercritical CO_2, *J. Angewandte Chemie Int. Ed.*, **2009**, 48, 4993-4995

45. Cummings, S., Xing, D., Enick, R., Rogers, S., Heenan, R., Grillo, I., Eastoe, J., Design Principles for Supercritical CO_2Viscosifiers, *Soft Matter*, **2012**, 8(26), 3044-3055